Journal of Hydrology 510 (2014) 164–181

Contents lists available at ScienceDirect

Journal of Hydrology

journal homepage: www.elsevier.com/locate/jhydrol

Evaluation of bed load transport formulae in a large regulated gravel bed river: The lower Ebro (NE Iberian Peninsula)

Raúl López [a,*], Damià Vericat [b,c,d], Ramon J. Batalla [b,c,e]

[a] Department of Agricultural and Forest Engineering, University of Lleida, Av. Alcalde Rovira Roure, 191, E-25198 Lleida, Catalonia, Spain
[b] Department of Environment and Soil Sciences, University of Lleida, Av. Alcalde Rovira Roure, 191, E-25198 Lleida, Catalonia, Spain
[c] Forest Science Center of Catalonia, E-25280 Solsona, Catalonia, Spain
[d] Institute of Geography and Earth Sciences, Aberystwyth University, Ceredigion SY23 3DB, Wales, UK
[e] Catalan Institute for Water Research, H2O Building, E-17003 Girona, Catalonia, Spain

ARTICLE INFO

Article history:
Received 5 June 2013
Received in revised form 1 October 2013
Accepted 7 December 2013
Available online 16 December 2013
This manuscript was handled by Konstantine P. Georgakakos, Editor-in-Chief, with the assistance of Ehab A. Meselhe, Associate Editor

Keywords:
Bed load formulae
Bed load transport
Gravel bed-river
Armored bed river
River Ebro

SUMMARY

This paper tests the predictive power of 10 bed load formulae against bed load rates obtained for a large regulated river (River Ebro) the armor layer of which is subject to repeated cycles of break-up and reestablishment. The theoretical principles of two of the 10 formulae explicitly include the effects of river bed armoring. The results obtained showed substantial differences in equation performance but no evident relationship between predictive power and theoretical approach (e.g., discharge, stream power and probability) was found. Overall, the predictive power of the tested formulae was relatively low. The average percentages of predicted bed load discharge that did not exceed factors of 2 ($0.5 < r < 2$) and 10 ($0.1 < r < 10$) in relation to the observed discharge were 19% and 57%, respectively (where r is the discrepancy ratio between the predicted and observed values). In particular, the formulae of Yang (1984) and Parker et al. (1982) presented the better levels of agreement with the observed bed load discharges. The bed load rating curve for the lower Ebro showed a similar degree of agreement to the best-performing formulae. However, its predictive power was limited because only flow discharge acts as an independent variable and river bed dynamics, such as armoring cycles, are not contemplated.

1. Introduction

Bed load is the part of the bed material that moves episodically during floods, either in traction (in rolling or sliding motion), or in saltation in the river channel. It controls the three-dimensional morphology of rivers and, in consequence, many fluvial research and management applications require estimates of bed load. Bed load transport is a highly variable phenomenon, both in space and time. This variability is reflected in the functional relations that link flow intensity to bed load. Such relations have an uncertainty that can be placed at some orders of magnitude (Gomez and Church, 1989). The origin of this lies partly in the highly local and unsteady nature of the driving forces but is also linked to changing rates of upstream sediment supply and to the composition and structure of the river bed (Wilcock, 2001; Di Cristo et al., 2006; Greco et al., 2012).

The main reason for development of bed load equations is the need to predict and plan in fluvial environments, and not only for engineering purposes. Unfortunately, the collection of high-quality bed load transport data is an expensive and time-consuming task, and for many practical purposes recourse is made to a bed load transport formula (Gomez, 2006). Within this context, numerous bed load transport formulae have been developed over a century with the main purpose of predicting bed load, overcoming the inherent variability of sediment transport together with the uncertainties and difficulties associated with sampling. Formulae cover a wide range of sediment sizes and hydraulic conditions. These formulae are based on the premise that specific relations exist between hydraulic variables, sedimentary conditions, and rates of bed load transport (Gomez and Church, 1989). Most of these models have been derived from flume experimental data (e.g., from early studies such as Gilbert, 1914; Kramer, 1934; Casey, 1935; USWES, 1935; Shields, 1936; Chang, 1939; and lately Hamamori, 1962) under steady and uniform flow conditions, rather than from observations of natural flow and transport. Few formulae derive from field measurements (e.g., Schoklitsch, 1950; Rottner, 1959; Parker et al., 1982; Bathurst, 2007). Inherent bed load transport variability, the changing sedimentary conditions of the river bed and sampling efficiency are all key components that affect the performance of equations. Equations are usually calibrated to

* Corresponding author. Tel.: +34 973 70 28 20.
E-mail addresses: rlopez@eagrof.udl.cat (R. López), dvericat@macs.udl.cat (D. Vericat), rbatalla@macs.udl.cat (R.J. Batalla).

0022-1694/$ - see front matter © 2013 Elsevier B.V. All rights reserved.
http://dx.doi.org/10.1016/j.jhydrol.2013.12.014

Notation

a	dimensionless coefficient
A_{gr}	threshold of mobility
C	coefficient
C_s	total bed-material concentration, ppm by weight
D_i	particle size of percentile i, m
D_{ir}	reference value of D_i, m
D_{is}	particle size of percentile i of subsurface material, m
D_{gr}	non-dimensional sediment size, m
D_m	arithmetic mean diameter of sediment, m
F_1	adimensional parameter of fall velocity
F_{gr}	sediment mobilization parameter
g	gravitational acceleration, m s^{-2}
gr	modified geometric mean value of r
gwr	weighted variation of gr
G_{gr}	dimensionless transport rate
k	Manning coefficient of roughness associated with skin friction only, s $m^{-1/3}$
k'	Manning coefficient of total roughness, s $m^{-1/3}$
m	exponent
mr	mean of discrepancy ratio (r)
mlr	mean of logarithm of discrepancy ratio (r)
mq_{sp}	minimum value of q_{sp}
n	transition parameter
N	number of data
Q	water discharge, m^3 s^{-1}
q_c	critical water discharge per unit width, m^3 s^{-1} m^{-1}
q_{c2}	critical water discharge per unit width for transport as the armor layer breaks up, m^3 s^{-1} m^{-1}
q_s	bed load discharge in weight per unit width, N s^{-1} m^{-1}
q_{sm}	bed load discharge in mass per unit width, kg s^{-1} m^{-1}
q_{so}	observed bed load discharge per unit width, N s^{-1} m^{-1}
q_{sp}	predicted bed load discharge per unit width, N s^{-1} m^{-1}
q_{sr}	reference value of q_{sm}, kg s^{-1} m^{-1}
q_{stv}	total bed-material load discharge in volume per unit width, m^3 s^{-1} m^{-1}
q_{stw}	total bed-material load discharge in weight per unit width, kp s^{-1} m^{-1}
q_{sv}	bed load discharge in volume per unit width, m^3 s^{-1} m^{-1}
q_*	dimensionless volumetric bed load transport rate per unit width
r	discrepancy ratio (q_{sp}/q_{so})
rw	weighted value of r
R	hydraulic radius, m
S	bed or channel slope, m m^{-1}
U_*	shear velocity, m s^{-1}
V	mean flow velocity, m s^{-1}
V_c	critical mean velocity, m s^{-1}
w_s	fall velocity of sediment, m s^{-1}
W^*	dimensionless bed load
y	mean flow depth, m
y_r	reference value of y, m
ϕ_i	excess Shields stress
γ	specific weight of water, N m^{-3}
γ_s	specific weight of sediment, N m^{-3}
ν	kinematic viscosity of water, m^2 s^{-1}
ρ	density of water, kg m^{-3}
ρ_s	density of sediment, kg m^{-3}
τ	mean shear stress, N m^{-2}
τ_*	Shields number
τ_i^*	Shields stress for D_{is}
τ_{ri}^*	reference value of τ_i^*
ω	stream power per unit bed area, kg s^{-1} m^{-1}
ω'	stream power per unit weight of fluid, m s^{-1}
ω_c	critical unit stream power, kg s^{-1} m^{-1}
$(\omega - \omega_c)_r$	reference value of excess stream power, kg s^{-1} m^{-1}

specific conditions used to derive them; these may be equilibrium conditions in the case of flume studies, but this is less likely for equations based on field data.

Since the initial comparison made by Johnson (1939) there have been several assessments of the performance of bed load transport formulae using both field and laboratory data (e.g., Shulits and Hill, 1968; White et al., 1973; Carson and Griffith, 1987; Yang and Wan, 1991; Chang, 1994; Reid et al., 1996; Batalla, 1997; Martin, 2003; Martin and Ham, 2005). Gomez and Church (1989) undertook one of the most complete evaluations of bed load formulae and noted that there are more bed load formulae than reliable data to test them (Martin, 2003). These authors concluded that no formula performs consistently well; this can be attributed to the limitations of the test data and to the constraints of the test and the physics of the transport phenomenon. The results of analyses of the performance of these equations have been published elsewhere. For example, even in the best performing equations evaluated by White et al. (1975) fewer than 70% of the predicted sediment transport rates lay between half and twice the observed values. Andrews (1981) showed that the best equations for predicting bed-material discharges, within a range of half to twice the observed values, lay between 60% and 79% of the observations. Later, Batalla (1997) corroborated that the degree of accuracy between observed and predicted values varies greatly between one formula and another. He reported that the percentage of observations in which the discrepancy ratio between observed and computed values had a value of between 0.5 and 2 ranged from 25% (van Rijn) to 38% (Brownlie), 52% (Meyer-Peter and Müller), 65% (Engelund and Hansen), and 68% (Ackers and White). Most evaluations conclude with a recommendation or representative formula, but no universal relationship between bed load discharge and hydraulic conditions has yet been established (Habersack and Laronne, 2002). According to Wilcock (2001) the lack of field data to test bed load performance and to analyses bed load transport complexities (e.g., variability) are identified as the key reasons why we cannot expect to obtain high predictive power of equations under selected conditions. Testing and verifying formulae in large regulated rivers poses an additional challenge that has not been generally treated in the literature. We specifically refer here to bed armor condition and its periodic break-up and reformation; these are not exclusive phenomena of rivers downstream from dams, since many natural gravel-bed rivers also show this behavior; but regulated rivers may exhibit more extreme conditions of supply limitation and armor development. In addition, due to channel dimensions and flow magnitude, large rivers offer less opportunity to obtain direct field data; field information on such large systems is, in general, sparse and scarce. Finally, regulated rivers are often subject to management actions, such as the release of periodical flushing flows that may exacerbate channel adjustments (e.g., Batalla and Vericat, 2009); those actions should preferably be planned based on empirical data (in this case bed load and riverbed dynamics) that soundly informs modeling, design, and implementation and re-evaluation avoiding, this way, completely blind engineering operations. Within this context, this paper principally aims to assess the predictive power of a series of bed load formulae tested against bed load transport rates obtained for a large

regulated gravel bed river. Field data were obtained in the lower River Ebro, downstream from the largest dam complex in the basin, for the period 2002–2004. This river undergoes cycles of break-up and reestablishment of its armor layer; this process has been contemplated in the analysis, but for a complete description, see Vericat and Batalla (2006) and Vericat et al. (2006a). Special attention has therefore been devoted to studying the performance of formulae under different armoring conditions; with the objective of informing users of these equations in rivers of similar characteristics where bed load data is unavailable. The novelty of this investigation relies on the facts that we account for the textural evolution of bed sediments during the study period, the choice of input grain size (surface vs. subsurface), and the armoring state. In particular, we show that undertaking analysis of equation performance as a function of the input grain-size is necessary as an important factor controlling predicted results. We also present how the observed scatter in transport rates can be reduced by accounting for textural evolution and armoring state, which suggests that these factors should be accounted for when predicting transport rates.

2. Study reach and field measurements

2.1. The lower Ebro

The annual runoff of Ebro River basin is highly dependent of mountain regions: the mountain area only represents about 30% of the total surface area of the Ebro basin but it is responsible for nearly 60% of its mean annual runoff (López and Justribó, 2010). The Ebro basin is extensively regulated by reservoirs: almost 190 large dams regulate 67% (≈7700 hm^3) of the river's mean annual runoff. The largest reservoir complex is located in the lower course of the river and was closed in 1969. It is comprised by three dams: Mequinenza, Ribarroja and Flix. Together, they impound 1750 hm^3 of water (13% of the basin's annual water yield). Frequent floods (i.e., Q_2–Q_{25}, where Q_i is the discharge associated with an i-years recurrence interval) have been reduced by 25% on average (Batalla et al., 2004), while large floods are no longer observed along this reach.

Flow hydraulics and sediment transport were regularly and continuously monitored during floods at the Mora d'Ebre Monitoring Section (hereafter MEMS) during the period 2002–2004. This section of the river has a channel width of 160 m and is located 27 km downstream from the Flix Dam. Along this reach, the river flows as a single, low-sinuosity channel. The mean longitudinal channel slope is 8.5×10^{-4}. During the study, the median surface river bed particle size D_{50} (where D is the size of the percentile i of the grain size distribution) in a gravel bar nearby MEMS ranged between 33 and 50 mm, while median subsurface size (D_{50s}) ranged from 19 to 21 mm. According to these values the mean armoring ratio ranges between 1.6 and 2.6 (armor ratio is estimated as the quotient between the surface and subsurface median particle size, as per Parker et al., 1982).

The 2002–2003 and 2003–2004 study periods were average hydrological years in terms of both the pre-dam and post-dam flow records (Vericat and Batalla, 2006). The mean discharge was 415 $m^3\ s^{-1}$ for the period 2002–2003 and 465 $m^3\ s^{-1}$ for 2003–2004. Several floods (some of which were natural and some of which were flushing flows for channel maintenance (see Batalla and Vericat, 2009)) occurred during the study period and almost all of them were monitored for sediment transport. The maximum recorded discharge during the study period occurred in February 2003 and reached 2500 m^3/s (with return period of 8 years, estimated from the post-dam flow series at the downstream Tortosa gauging station); so we consider this event to be a large flood in the context of historic flood distribution i.e., largest recorded flood occurred in 1907 and attained an estimated peak of 12,000 m^3/s. The entire bed load is trapped in the upstream reservoir complex. As a result, the river does not receive any coarse-grained bed load fractions from further upstream. However, the river partially maintains its bed load transport capacity since floods still have enough competence to entrain river bed sediments downstream from the dam (Vericat and Batalla, 2006).

2.2. Field measurements

Here we present a summary of the field methods used to measure discharge, to characterize river bed sediments and to measure bed load at MEMS. Field measurements have already been extensively described by Vericat and Batalla (2006) and Vericat et al. (2006a, 2006b), and further referred in Batalla and Vericat (2009).

Flow was calculated at the monitoring section by routing hydrographs from an upstream gauging station operated by the Ebro Water Authorities (Ascó, n. 163, 15 km upstream); and further compared with discharges in Tortosa (n. 27, 49 km downstream). Discharge measurements were used to corroborate flood hydrographs. Velocity of the flow was measured from the MEMS bridge by means of an OTT C31 current meter which was attached to a cable-suspended US DH74 sampler. Eleven velocity profiles were obtained for instantaneous discharges between 750 and 2160 $m^3\ s^{-1}$. Mean velocities were calculated from velocity profiles and subsequently used to verify routed discharges from the upstream gauging station.

For the purposes of this paper, we used the bed material grain size distribution (i.e., surface and subsurface) that was obtained from the closest exposed bar to MEMS. The bar is located less than 500 m downstream (a distance equivalent to four times the mean channel width). It is the nearest open and accessible gravel deposit to the measuring site; we consider it fully representative of the grain-size distribution of the active sediments in the river (for more details on Ebro's grain size distribution see Vericat et al., 2006a). Additionally, inactive sediment, which was differentiated by the vegetation cover, was avoided because it may have little relation with the current river regime. Bed material sampling was performed on two occasions in relation to the river's armoring cycle (see methods and results sections for a complete description and discussion): (a) Bed Material I (hereafter BMI) was carried out in summer 2002, i.e., just before the beginning of the 2002–2003 hydrological year; and (b) Bed Material II (hereafter BMII) was undertaken in summer 2003, again just before the beginning of the 2003–2004 hydrological year. The coarse surface layer was characterized using the pebble count method (Wolman, 1954; Rice and Church, 1996) in the BMI characterization. A considerable proportion of fine material (i.e., particles finer than 8 mm) was found at the bed surface in summer 2003 (i.e., BMII characterization); the surface material was then sampled using the area-by-weight method (Kellerhals and Bray, 1971). This method offers the possibility of obtaining an accurate determination of the percentage of fine material as this parameter is known to be underestimated by the pebble count method. In both campaigns, the surface material was differentiated from the underlying sediment using spray paint (Lane and Carlson, 1953). The sampled area was then calculated following the Fripp and Diplas (1993) formula: $A = 400(D_{max\text{-}s})^2$, where A is the area (m^2) of the river bed surface that has to be painted and sampled and $D_{max\text{-}s}$ is the b-axis (m) of the exposed particle of maximum size. Area-by-weight samples were converted to volumetric values (Kellerhals and Bray, 1971) applying a conversion factor of −0.5 (for more details, see Vericat et al. (2006a)). The subsurface material was sampled using the volumetric method after first removing the surface layer. The depth of the subsurface layer was around 0.3 m; this value lay within the range for the

active layer that was observed during the study period. The largest particle found in the subsurface layer did not exceed 1% of the sample weight (as per Church et al., 1987). For full coverage of river bed material sampling in the River Ebro, including a discussion about the precision of measurements and variability in bed material for the whole reach see Vericat et al. (2006a). Combined bed grain size distributions were generated according to Fripp and Diplas (1993) and Rice and Haschenburger (2004). Grain size distributions of the bed material are presented in Fig. 1 and Table 1. Fig. 1 shows that particles finer than 1 mm are not present in the bed surface, whereas in the subsurface layer they represent less than 5%, implying that the potential impact of the sizes transported in suspension on bed load is negligible.

Bed load database encompassed 174 samples (124 of which were obtained during the 2002–2003 hydrological year, with the other 50 being obtained in 2003–2004). Around 96% of the total flow range was sampled for bed load during the whole study period. Bed load was sampled using a cable suspended Helley–Smith sampler with a 152 mm intake and an expansion ratio of 3.22. Bed load sampling did not exceed 5 min and it was carried out using an automatic crane. Samples were collected in a single vertical (i.e., channel center). Vericat and Batalla (2005) provided an assessment of the temporal and spatial variability of bed load transport during steady flow conditions. Results indicated that bed load sampling at that single vertical represented exactly the weighted mean bed load of the section in 40% of the samples; whereas in the other occasions the ratio between cross-sectional rates and bed load at the vertical ranged from 4 to 6. We consider this sufficient to warrant representation of the total bed load discharge by measurements at the vertical (Vericat and Batalla, 2006).

As previously mentioned, the D_{50} of the gravel bar nearby MEMS ranged from 33 to 50 mm, while the largest particles found on the surface measured 117 mm; thus, the 152 mm Helley–Smith should have ensured the efficient sampling of the bed load for almost all the different grain size classes (for more details on the variability of bed load and sampling reliability see Vericat and Batalla, 2006, and Vericat et al., 2006b).

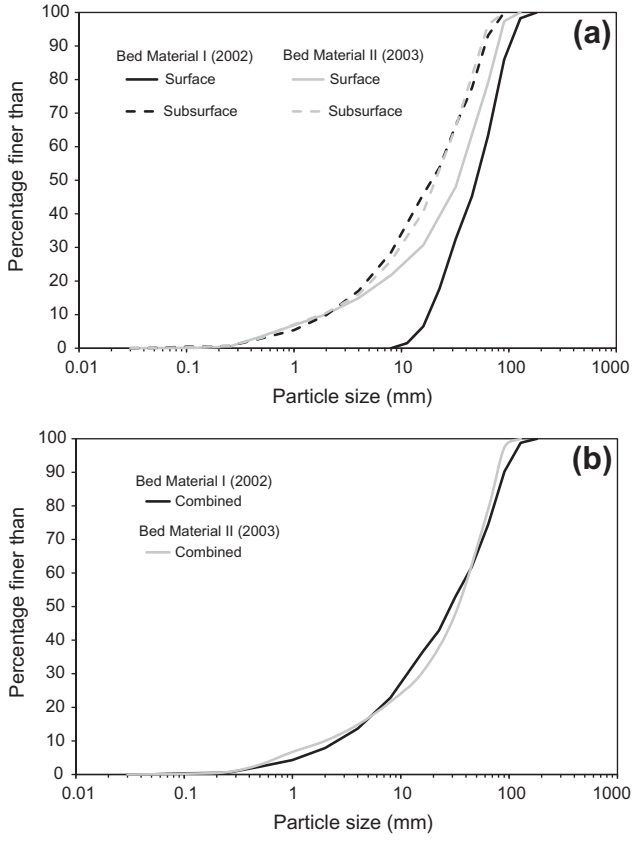

Fig. 1. Bed material grain-size distributions at an exposed bar 500 m downstream from the MEMS: (a) surface and subsurface grain-size distributions of Bed Material I (BMI, obtained in 2002) and Bed Material II (BMII, obtained in 2003), and (b) combined distribution (surface and subsurface materials) for each sampling period (BMI and BMII). Statistics are summarized in Table 1 (see methods in the text).

3. Bed load formulae

A set of 10 bed load transport formulae were selected. Details of the selected formulae are presented in Table 2 and fully described in Appendix A. The main and most common criterion for selection was that they were commonly applied to gravel-bedded rivers with moderate to low slope (e.g., <1%). Specifically, the formula that presented an experimental range strictly applicable to the data obtained for the lower course of the Ebro was the one developed by Bathurst (2007) (hereafter Bt). Moreover, according to the characteristics of the formulae presented in Table 2, the size of the bed material in the lower Ebro fits within the experimental range reported by Bagnold (1980) and Parker et al. (1982) (hereafter referred to as B and P–K–M, respectively). Appendix A presents the formulae as they have been applied in the present study. Bed load discharge has been calculated in dry weight per unit width (i.e., q_s, where the fundamental dimensions are [MT^{-3}] expressed in SI units as N s^{-1} m^{-1}).

Most of selected formulae in this study were derived from flume experiments, in which lateral variation of hydraulic variables were not critically important. According to Ferguson (2003) this type of formulae can lead to underestimate bed load fluxes if applied to channel where there is a substantial lateral variation in flow hydraulics (e.g., shear stress). However, in our case study, the river shows a hydraulically wide channel (i.e., high values of the ratio free surface width/mean flow depth). This implies that, in practical terms the difference between at-a-section mean values of hydraulic variables and the values of those variables at the vertical where bed load was sampled is small. For instance, the mean difference between mean flow depth and at-a-section and at the sampling vertical was ≈10% (with a maximum value of 15% during high discharges); whereas the mean difference between at-a-section and at-a-vertical mean velocity was 7% (with a maximum

Table 1
Grain size percentiles of surface, subsurface and combined river bed material observed in the lower Ebro river (500 m downstream from the monitoring site; see Fig. 1 for the complete grain size distributions).

Grain size, D_i (mm)	Bed Material I (BMI)[a]			Bed Material II (BMII)[c]		
	Subsurface	Surface	Combined[b]	Subsurface	Surface	Combined[d]
D_{35}	10	34	15	12	19	19
D_{40}	13	39	19	15	23	23
D_{50}	19	50	29	21	33	33
D_m	26	55	40	26	38	38
D_{84}	52	88	79	48	70	70

[a] Sampling was conducted before the flood season; BMI: characterization performed in 2002, at the beginning of the 2002–2003 hydrological year.
[b] Combined grain-size distribution has been calculated according to Fripp and Diplas (1993) and Rice and Haschenburger (2004).
[c] BMII: characterization performed in 2003, at the beginning of the 2003–2004 hydrological year.
[d] Fines were significant on the surface in summer 2003. Surface material was sampled by means of the area by weight approach, a sample that represents the full range of sizes in the bed. Percentiles for the surface and combined distributions are almost identical because the weight of the subsurface material on the combined one.

Table 2
Characteristics of the selected bed load transport formulae.

Formula	Name or reference	Load	Theoretical approach	Environment of the data	N[a]	Experimental range
S	Schoklitsch (1950)	Bed load	Discharge	Flume, field	–	$0.3 < S\ (\%) < 10$
MP–M	Meyer-Peter and Müller (1948)	Bed load	Shear stress	Flume	251	$0.040 < S\ (\%) < 2.0$ $0.38 < D_m$ (mm) < 28.65
W–P	Wong and Parker (2006)	Bed load	Shear stress	Flume	168	$3.17 < D_m$ (mm) < 28.65
E–B	Einstein–Brown, Brown (1950)	Bed load	Probabilistic	Flume	–	$0.3 < D_{50}$ (mm) < 28.6
A–W	Ackers and White (1973), Ackers (1993)	Total load[b]	Stream power	Flume	≈1000	$0.04 < D$ (mm) < 4 $F < 0.8$
B	Bagnold (1980)	Bed load	Stream power	Flume, field	–	$0.3 < D_{50}$ (mm) < 300
Y	Yang (1984)	Total load[b]	Stream power	Flume	167	$2.5 < D$ (mm) < 7.0
R	Rottner (1959)	Bed load	Regression	Flume, field	≈2500	$0.31 < D_{50}$ (mm) < 15.5
P–K–M	Parker et al. (1982)	Bed load	Probabilistic, equal mobility	Field	–	$D_{50s} < 28$ mm
Bt	Bathurst (2007)	Bed load	Discharge	Field	≈600	$0.048 < S\ (\%) < 4.8$ $12 < D_{50}$ (mm) < 146 $30 < D_{84}$ (mm) < 540 $1.52 < D_{50}/D_{50s} < 11$

[a] Number of calibration data.
[b] Total bed-material load.

value of 18% during high discharges). Such flow differences may imply the presence of bedforms, therefore higher variability in bed load rates could be expected; however, no field evidences are available to critically analyze this process.

Some of the selected formulae (e.g., Yang (1984) (hereafter Y) and Parker et al. (1982)) explicitly recommended the estimation of fractional bed load rates. This recommendation was not followed here as we sought to facilitate comparisons between formulae. For the same reason we also avoid selecting other formulae (e.g., Parker, 1990) that require fractional-based bed load transport calculation. Eight of the chosen formulae specifically estimate bed load transport. The other two, those by Ackers and White (1973) (hereafter A–W) and Y, permit estimating total bed-material load. However, in the case of the A–W formula, when the dimensionless particle diameter exceeds a given threshold, as happens in the Ebro, it is only used to estimate bed load rates and not bed material transport. In addition, given that the median diameter of the study reach exceeds the upper application limit of the Y formulae (i.e., 7 mm) we assume that the gravel concentration in the suspended load in relation to bed load is negligible in these estimates.

A number of theoretical bases for bed load calculation are represented by the selected formulae. All the main approaches, which include those represented by discharge, energy slope or shear stress, probability, stream power, regression and equal mobility, are found in the selected equations (Table 2). The discharge approach adopts critical water discharge per unit width (q_c) as the criterion for determining particle entrainment and is based on basic field parameters such as sediment size and river channel slope. The shear stress approach is based on the difference between applied and critical shear stress. The stream power approach relates bed load transport to power per unit bed area ($\omega = \rho \cdot V \cdot y \cdot S$, where ω is the stream power per unit bed area (in mass units), ρ is the density of the water, V is the mean flow velocity, y is the mean flow depth, and S is the energy slope) (Bagnold, 1980); or to the power available per unit weight of fluid ($\omega' = V \cdot S$, where ω' is the stream power per unit weight of fluid) (Yang, 1973, 1984). In contrast to these deterministic models, the probabilistic approach relates bed load to fluctuations in the turbulent flow; furthermore, in the case of the Einstein–Brown (Brown, 1950) formula (hereafter E–B) no fixed entrainment criterion is defined. The regression approach is typically based on the statistical fitting of the parameters of an equation obtained by means of dimensional analysis. Finally, the equal mobility approach assumes that all grain size ranges are of approximately equal transportability once the critical condition for breaking the armor has been exceeded.

Only two of the selected formulae (i.e., P–K–M and Bt) explicitly include in their theoretical principles the influence of armoring on bed load transport. The other formulae are based on data that were mostly derived from flume experiments that did not take into account the effects of armoring on bed load transport. This poses a serious question relating to selection of the most appropriate river bed particle size (i.e., surface or subsurface) for the subsequent evaluation of the formulae; the bed material size used to evaluate the formulae selected in this study is extensively described in Section 4.3.

4. Data treatment

To begin, raw bed load and water discharge data were correlated. Data were subsequently divided according to periods in which bed-material was sampled (see next Sections 4.1 and 4.2. for a more detailed explanation). Later, in order to create the database against which the formulae were finally tested, the complete data set was broken according to two different criteria: bed material characteristics and the degree of armoring. Data were subsequently grouped by discharge bins; this reduced the scatter and increased the goodness of the relationship between bed load and discharge. A detailed explanation of the data treatments is provided in the following sections and schematically simplified in Table 3.

4.1. Raw data

A very low degree of correlation was observed between the measured q_s and Q in a log-transformed least-squares best-fit regression (Fig. 2a). Often this poor correlation may be exacerbated by a narrow range of discharge observations. This is not the case of the Ebro where bed load was sampled from the very onset of motion (at ca. 600 $m^3\ s^{-1}$) to flood flows corresponding to a 3-year flood (close to 1600 $m^3\ s^{-1}$); under more than fifteen meters of water. In our case, as previously reported by Vericat et al. (2006a), this variability between q_s and Q can be mainly attributable to the distinct role played by sediment supply-availability and the role of bed armoring during the study period. The lower Ebro has a well-formed and dynamic armor layer. This layer is successively broken up and reestablished according to the magnitude of the flood. The magnitude of the bed load flux increases when the armor breaks up. This process is always driven by an increment in

Table 3
Schematic division of the data performed in this study. Two main analyses were performed: (a) based on the raw data and (b) based on data division. Data division was based on bed material characteristics and on the armor layer integrity.

Raw data			Data division		
Bed material samples, $N = 2$	Bed load samples, $N = 174$	Bed Material Division	Discharge classes, $N = 21$	Bed Material Division (BMD)	Armor Layer Division (ALD)
2002–2003					
Bed Material I (BMI)					
High magnitude floods	Sample 1	BMI	Q_1 ($Q_1 < 700$ m^3 s^{-1})	BMI	Unbroken Armor Layer (UAL)
	Sample 2		Q_2 (Q_1–Q_{1+j})		
	...		...		Broken Armor Layer (BAL)
	...		...		
	...		...		
	Sample 124		...		
2003–2004					
Bed Material II (BMII)			...		
Low magnitude floods	Sample 125	BMII	...	BMII	Reestablished Armor Layer (RAL)
	Sample 126		...		
	...		...		
	...		...		
	Sample 174		Q_n (Q_{1+k}–Q_{1+k+j})		

the supply of subsurface material to the bed load flux which in turn affects the texture of the moving material. When the magnitude of subsequent floods is not sufficient to entrain the whole range of particle sizes on the river bed, the armor reestablishes. The bed surface then becomes coarser and the bed load becomes more selective. Under such conditions, at a given discharge, not only can the magnitude of the bed load flux be very variable, but so too can the texture of the bed load. A full description of all of these processes is provided in Vericat et al. (2006a).

Table 3 summarizes the different data treatments followed in this study. Bed material was sampled on two occasions: Bed Material I (BMI in 2002) and Bed Material II (BMII in 2003) (Table 1). In order to study the influence of bed material on the relationship between bed load discharge and flow discharge, the complete data set was partitioned according to the periods in which the different bed materials were sampled. Two sets of bed load samples were therefore derived: (a) those collected between BMI and BMII ($N = 124$); and (b) those collected after BMII ($N = 50$). The bed load samples in (a) were called BMI, while those in (b) were referred to as BMII (Table 3). Both groups were plotted against discharge in Fig. 2b. The relationships in this figure show that the BMI bed load samples were the subset of samples that provided the majority of the scatter in the general relationship presented in Fig. 2a. The BMI samples corresponded to a combination of bed load samples that were obtained under different degrees of armoring (including no armoring).

The river bed is subject to cyclic incision and armoring processes that are related to flood magnitude (Vericat et al., 2006a). At the beginning of the study period, the armor layer was established (i.e., armoring ratio ≈ 2.6), while during the floods that occurred between BMI and BMII the armor was broken up as discussed in Vericat et al. (2006a). We hypothesize that during the process of breaking up the supply of sediment was highly variable and erratic due to partial disruption of the armor; thus controlling the high scatter observed for bed load. The pattern observed for the BMII samples was the more hydraulically driven, presenting less scatter and a clearer relationship with flow discharge (Fig. 2b). The bed material characterization obtained after the 2002–2003 winter floods that broke up the armor layer (i.e., Bed Material II in Table 1) indicated that the armoring intensity decreased (i.e., the armor ratio decreased to 1.6). More relatively fine material was available for the 2003–2004 winter floods. These floods were characterized by their relatively low magnitude compared with those of the previous year. Their competence was not sufficient to entrain all the bed particle sizes present on the bed; as a result, the armor layer had become re-established (i.e., mean armoring ratio increased to 2.3) by the end of the season (Vericat et al., 2006a). Worth to mention, that the mean net channel incision after high magnitude floods in 2002–2003 was 60 mm. Incision was minimal during low magnitude floods (i.e., Q_{1-2}) in the following period.

Taking into account the high variability of the instantaneous bed load rates and the complex dynamics observed on the river bed (which have been previously described), we decided to further break or divide the original database ($N = 174$; Table 4), following two independent criteria: (a) the characteristics of the bed material (i.e., Bed Material Division, BMD) and (b) the armor integrity (i.e., Armor Layer Division, ALD). Once these divisions had been made, the data were independently grouped by flow discharge class to minimize the degree of scatter and to facilitate comparisons with bed load formulae predictions (Table 3). More details about the data division applied can be obtained from Table 4. Note that the main objective of this paper is not to examine instantaneous bed load variability, but to assess and compare the predictive power of the selected formulae. The adopted data division is thus fully justified.

4.2. Data division

Bed load data for each division (i.e., BMD and ALD) were grouped following a discharge class division with range amplitude accounting for approximately 3% ($\approx$40 m^3 s^{-1}) of the total range of measured discharges (from 343 to 1555 m^3 s^{-1}). The scatter of the bed load rates was especially high for discharges of between 343 and 700 m^3 s^{-1}. Variability may be related to selective transport over the armored bed. The flow division criterion was therefore not applied to the cited interval and a single discharge class (<700 m^3 s^{-1}) was adopted. Overall, as no bed load data were present for the 1392–1433 m^3 s^{-1} class, the total number of discharge bins conforming the analysis was 21. Class values of q_s and the rest of the hydraulic variables (mean depth, mean flow velocity) were obtained as the means of all the values that constituted each discharge bin or class.

4.2.1. Bed Material Division (BMD)

By this division, two data sets were obtained: (a) all the bed load samples obtained between BMI and BMII, and (b) all the bed load samples collected after BMII (Table 3). All the samples in each

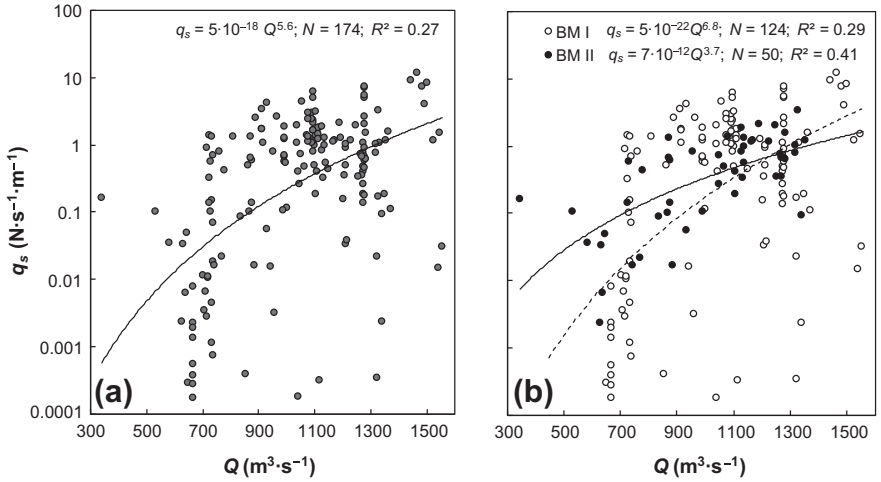

Fig. 2. Relation between observed unit bed load discharge and water discharge: (a) original database, and (b) original database divided by bed material: Bed Material I (BMI, bed load samples between summer 2002 and summer 2003) and Bed Material II (BMII, samples after summer 2003).

set were grouped in accordance with the discharge approach as outlined above. The result of this treatment was a data set composed of 19 samples for the BMI condition and 17 samples for BMII (Table 4). As previously explained, the number of samples did not reach 21 because no bed load data were presented for one of the discharge bins. This data set constitutes one of the two data groupings against which the bed load formulae were tested in this paper.

Fig. 3a shows the relationship between q_s and Q for subsets of the BMD. The degree of correlation of these relations was higher than those obtained for the curves presented in Fig. 2b, the data of which were not grouped by discharge class. However, in absolute terms, the predictive power of the function still remained limited and well below previously adopted reference values for non-linear i.e., power relationships (e.g., Barry et al., 2008).

4.2.2. Armor Layer Division (ALD)

A preliminary analysis of the texture of the bed load samples (Vericat et al., 2006a) and field observations showed that: (i) after the first flood in December 2002, the armor persisted; (ii) the floods registered in February and March 2003 broke up the armor layer; and (iii) the armor was reestablished during the November 2003, December 2003 and May 2004 flood events. The bed load data set was then divided in line with these considerations (Table 3). A total of three armor layer conditions were identified: (a) Unbroken Armor Layer (hereafter UAL), (b) Broken Armor Layer (hereafter BAL), and (c) Reestablished Armor Layer (hereafter RAL). All of the samples in each division were grouped according to the discharge approach described above. The result of this treatment was a data set composed of 9 samples for the UAL condition, and 15 and 17 samples, respectively, for the BAL and RAL conditions (Table 4). As previously stated, the number of samples did not reach 21 because no bed load data were presented for someone of the discharge bins. It is necessary to consider that the RAL data subset coincided with the BMII group in the Bed Material Division; this can be explained by the fact that all of the floods registered after the BMII bed characterization were classified as events in which the armor was reestablished. This data set constitutes the second of the two data groupings against which bed load formulae were tested in this study.

Fig. 3b shows the relationship between q_s and Q as a function of the armor integrity condition: UAL, BAL, and RAL. This figure shows better grouping and, certainly, correlations improved when this division was considered; however, for UAL and BAL the regression coefficients (R^2) are still poor. The BAL and UAL relations are at opposite extremes and clearly represent different sediment supply conditions. For a given discharge, a larger bed load discharge would be expected for BAL than for UAL conditions. The RAL condition represents an intermediate position, although it did not plot very far from the BAL relation (Fig. 3b).

4.3. Bed material input to formulae

Transport equations are sensitive to bed-material grain-size, which can differ by a factor of two or more between surface and subsurface values in armored channels. Many older bed load equations did not recognize different bed-material domains (i.e., surface, subsurface, combined) making unclear which grain-size should be used to drive transport predictions. Worth to mention that laboratory mixtures used to derive bed load transport from flume studies can be considered equivalent to the subsurface sediments typically found in the field, since they distinct input grain-size that are relevant for equation development and performance. Within this context, undertaking analysis of equation performance as a function of the input grain-size is useful, if not necessary, to further highlight its importance as a controlling factor of predicted results, as we do in this paper. The role of bed load texture (based on bed load samples) improving formulae prediction was shown by Habersack and Laronne (2002) emphasizing the sensitivity of model performance to bed material input. In our study, only 2 of the 10 tested formulae explicitly include in their theoretical principles the effects of river bed armoring: P–K–M and Bt (Table 2). For the remaining 8 formulae, different bed material feeding (or input) criteria were adopted in order to test the role of bed material on bed load predictions. Specifically, the following considerations were made when selecting the bed texture with which to run the analysis:

1. Bed Material Division (BMI and BMII data sets): (A) a first run of the formulae was conducted using the subsurface grain size distribution from the samples obtained in 2002 (i.e., BMI) and 2003 (i.e., BMII, see Table 1 for more details). A total of 36 predictions were obtained. (B) The formulae were subsequently run using the surface grain size distributions obtained for each period (i.e., BMI and BMII). As in the consideration (A), a total of 36 predictions were calculated.
2. Armor Layer Division (UAL, BAL and RAL data sets): in this case the texture inputs of the formulae were related to the armor condition for each data set. (A) Unbroken Armor Layer (UAL):

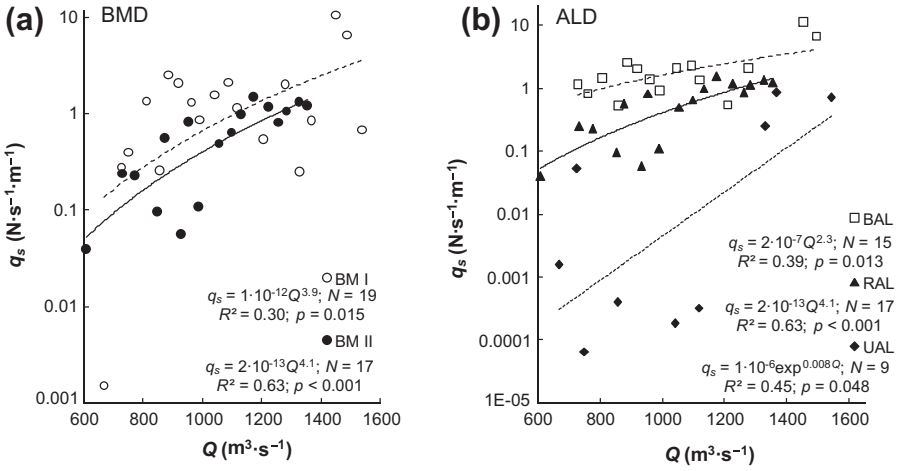

Fig. 3. Relation between average unit bed load discharge and water discharge. (a) Data divided by bed material (BMI and BMII) classes and grouped by discharge bins: Bed Material Division (BMD). (b) Data divided by armoring integrity and grouped by discharge bins: Armor Layer Division (ALD) (see Section 4.2 for more details about data sets grouping and division).

Table 4
Data division: number of data in each subset (see Section 4 for more details).

Original database	Data division						
	Bed material		Grouping discharges				
	Bed Material I	Bed Material II	Bed Material Division (BMD)		Armor Layer Division (ALD)		
			BMI[b]	BMII[c]	UAL[d]	BAL[e]	RAL[f]
N[a] = 174	N = 124	N = 50	N = 19	N = 17	N = 9	N = 15	N = 17

[a] Number of data.
[b] BMI, Bed Material I, river bed grain size distributions obtained in 2002.
[c] BMII, Bed Material II, river bed grain size distributions obtained in 2003.
[d] UAL, Unbroken Armor Layer condition.
[e] BAL, Broken Armor Layer condition.
[f] RAL, Reestablished Armor Layer condition.

the formulae were run using the surface grain size distribution obtained in BMI; (B) Broken Armor Layer (BAL): a combined grain size distribution for the BMI period was used. Surface and subsurface materials were combined in a single grain size distribution as described in Section 2.2 and can be seen in Fig. 1b; and, finally (C) Reestablished Armor Layer (RAL): the surface grain size distribution obtained during BMII was used as input for the formula texture. A total of 41 predictions were obtained (Table 4). It is worth mentioning that analysis based on the Armor Layer Division may provide a better understanding of the observed phenomena with greater explanatory power since it allows a more accurate adjustment of the grain size distribution in line with the particular conditions of each of the flood events analyzed.

The texture input in the P–K–M and Bt formulae, which explicitly include the effects of river bed armoring in their respective theoretical principles, requires further consideration. In both of these cases, the formula in question directly specify the (surface or subsurface) material required to predict bed load discharge i.e., P–K–M (only subsurface) and Bt (surface and subsurface). Moreover, these formulae can only be applied once the armor has been broken, a condition that is estimated by the formulae. These formulae will therefore only be applied for: (a) samples in BMI and BMII (Bed Material Division) that exceed the armor breaking condition estimated by the formulae, and (b) samples in BAL (Armor Layer Division) if the formulae predict that the armor will be broken.

It is widely acknowledge that textural evolution of the bed affects transport rates during and between floods (e.g., Parker and Klingeman, 1982; Dietrich et al., 1989; Parker, 1990; Vericat et al., 2006a; Turowski et al., 2011). However, few studies account for this variability when applying bed load transport equations and none examine such effects on equation performance. Although at a different temporal scale (i.e., annual instead of flood), our approach takes into account the variability of bed characteristics and its influence on formulae performance, by considering an Armor Layer Division: unbroken, broken and reestablishment conditions; a fact that reflects the progressive changes in bed surface grain-size.

5. Assessment of formulae performance

The predictive power of selected formulae was assessed and ranked by comparing observed (q_{so}) and predicted (q_{sp}) values of the unit bed load discharge. The main issues assessing formulae performance relate to (a) formulae that erroneously predict zero bed load transport, and (b) to the deviation between q_{so} and q_{sp} that typically span a large range of values (both in absolute (q_{so}–q_{sp}) and relative (q_{so}/q_{sp}) terms).

These issues were addressed in the following way. Incorrect zero predictions (i.e., $q_{sp} = 0$) may be obtained at low flow rates if the averaged predicted threshold value for particle entrainment is not exceeded. Zero bed load predictions are incompatible with many of the statistical indices commonly used to assess formulae performance. One frequent solution is the substitution of zero

predictions by a minimum value of bed load discharge (e.g., Barry et al., 2004, 2007; Recking, 2010). Occasionally, if the proportion of zero predictions is significant, some indices may end up as functions of the minimum adopted values of q_{sp} rather than as real indicators of formula performance (e.g., Barry et al., 2007). In this study, we took a minimum value of q_{sp} (mq_{sp}) adapted to the minimum observed value of q_{so} for each of the data subgroups (BMD and ALD), but based on a sensitivity analysis undertaken for the different statistical indices. We examined the effect of a wide variation of mq_{sp} (i.e., between 1×10^{-9} and 1×10^{-2} N s^{-1} m^{-1}) for all the statistical indices. Although these indices are properly introduced further in the text, this analysis illustrated as equations showed progressively better adjustment with the increase of the mq_{sp} value adopted for predictions 0. It is worth to mentions, the selected value of mq_{sp} only begins to affect the arithmetic mean of the discrepancy ratio (i.e., *mr*, index further introduced) for almost all the equations when mq_{sp} was greater than a given value; a value that was adopted for selecting mq_{sp} for each data division. Specifically, in the case of the Bed Material Division database the critical value of mq_{sp} was around 1×10^{-3}N s^{-1} m^{-1}, representing the 65% of the minimum q_{so}, which was exceeded by 93% of the values in the original dataset ($N = 174$). In the case of the Armor Layer Division database, however, the critical value of mq_{sp} was around 4×10^{-5}N s^{-1} m^{-1}, a value that represented 62% of the minimum q_{so}, which was exceeded by 99% of the values in the original dataset.

Several statistical indices and graphical methods were used to assess the performance of the different formulae. These indices are based on the discrepancy ratio (r) between the predicted and observed values ($r = q_{sp}/q_{so}$). The range of this ratio is (0, +∞). In bed load studies r can span a large range of values: frequently two or more orders of magnitude (e.g., Duan et al., 2006; Recking, 2010). Statistical comparisons should therefore also include log transformations and indices that are less sensitive to extreme values.

First, we calculated the percentage of q_{sp} that did not exceed a factor of 2 ($0.5 < r < 2$), 5 ($0.2 < r < 5$) and 10 ($0.1 < r < 10$) in relation to q_{so}. The arithmetic mean of r (*mr*) was also used:

$$mr = (1/N)\sum_{i=1}^{N} r_i \quad (1)$$

where r_i is the i value of r, and N is the number of data. This value is in the range (0, +∞), with values close to 1 indicating less discrepancy. The arithmetic mean of $\log r$ (*mlr*) was also used:

$$mlr = (1/N)\sum_{i=1}^{N} \log r_i \quad (2)$$

where r_i is the ith value of r, and N is the number of data. This value is in the range (−∞, +∞), with values close to 0 indicating less discrepancy. A modified type of geometric mean value of r (*gr*) (Habersack and Laronne, 2002) was also used:

$$gr = (r_1 r_2 \cdots r_i \cdots r_N)^{1/N} \quad (3)$$

where the reciprocal value is used if $r_i < 1$, ensuring that $gr \geqslant 1$. This value is in the range (1, +∞), with low values indicating the smallest discrepancies. A weighted variation of the *gr* index (*gwr*) (Habersack and Laronne, 2002) was also used:

$$gwr = (rw_1 rw_2 \cdots rw_i \cdots rw_N)^{1/N} \quad (4)$$

where *rw* is a value of r weighted by the power of the observed bed load discharge ($rw = r^{q_{so}}$) and where the reciprocal value is used if $rw_i < 1$, ensuring that $gwr \geqslant 1$. This value is in the range (1, +∞), with low values indicating the smallest discrepancies between q_{sp} and q_{so}.

We also graphically examined (at the log scale) the deviation between q_{so} and q_{sp} for each bed load transport value and we analyzed the distribution of the discrepancy ratio (r) using a box-plot diagram at the logarithmic scale. The ranking of the performances of different formulae may vary according to the statistical properties of the indices in question (e.g., Habersack and Laronne, 2002; Barry et al., 2007). For instance, the *mr* index is more sensitive to r values larger than 1 (i.e., a value of $r = 10$ weighs more in the *mr* computation than a value of 0.1, despite the fact that both represent a deviation of one order of magnitude with respect to the symmetry axes $r = 1$). The *mr* index is therefore less sensitive to the proportion of zero predictions and also to the minimum adopted value of q_{sp}. In contrast, in the *mrl* index, errors of equal magnitude weigh the same, independently of their relative positions with respect to the symmetry axes $\log r = 0$ (e.g., $r = 10$ and $r = 0.1$). It is therefore more sensitive to the proportion of zero predictions and to the minimum adopted value of q_{sp}. A limitation of *mlr* is that $\log r$ values of the same magnitude and opposite signs cancel each other out, yielding $mlr = 0$. This index is therefore more sensitive to small but asymmetrical deviations (e.g., if $r_1 = 1.5$ and $r_2 = 2$ then $mlr = 0.24$) than to larger symmetrical deviations (e.g., if $r_1 = 0.01$ and $r_2 = 100$ then $mlr = 0$). Furthermore, *gr* is less sensitive than *mr* to high values of r (i.e., $r \gg 1$) because it is based on the geometric mean; however, it is more sensitive to zero predictions, since a reciprocal value is taken if $r < 1$. Finally, the *gwr* index is more sensitive to deviations of large q_{so} values. Previous works (e.g., Barry et al., 2007) conclude that, given the potential bias of error index, there is no perfect method for assessing equation performance, especially in those cases that allows for inclusion of incorrect zero predictions.

The performance of the formulae is ranked for each index. The global performance of the formulae is assessed on the basis of a combination of three different criteria: (a) the relative position for each index, (b) the frequency with which the formulae are located in the top five positions, and (c) the ratio between the index value obtained using a given formula and the lowest index value (i.e., this last value is determined by the lowest ranked formula). We also present the log scale comparison between q_{sp} and q_{so} for the Bed Material and Armor Layer divisions. Finally, we present a box plot in log scale corresponding to the distribution of the discrepancy ratio (r) for: (a) BMD (fed with subsurface bed material), (b) BMD (fed with surface bed material), and (c) ALD divisions.

6. Bed load regime

A full description of the flow and bed load regime during the period 2002–2004 was reported by Vericat and Batalla (2006); hence, only a brief summary is presented here to contextualize the main results of this paper. Bed load was sampled during almost all of the floods recorded during that period. The mean bed load rate was 1.36 N s^{-1} m^{-1} in 2002–2003 (i.e., BMI) and 0.65×10^{-1} N s^{-1} m^{-1} in 2003–2004 (i.e., BMII). Worth to notice that that bed load rates during the first period show a highly variable pattern for a given discharge (Fig. 2b), contributing to a high scatter in the plot. Maximum rates were recorded in 2002–2003, with an instantaneous maximum value of 11.8 N s^{-1} m^{-1} (for further details, see Vericat and Batalla (2006)).

Bed load texture was markedly different in the two periods. The median bed load particle size in the samples collected during the period 2002–2003 varied from 1 to 72 mm, while for 2003–2004 this range decreased to 4–44 mm, showing a more selective transport range. The upper limits of both ranges corresponded to the D_{70} and D_{65} of the bed surface grain size distribution obtained in 2002 and 2003 respectively (Fig. 1). The lower limit was not present in

the surface sediments sampled in 2002 and represents the D_{15} of the 2003 distribution.

The original database ($N = 174$) was grouped according to the previously reported discharge class division in order to define a bed load rating curve for the lower Ebro. Note that in this case data were not divided according to any specific bed material or armor integrity criteria. The corresponding bed load transport model is:

$$q_s = 4 \times 10^{-10} Q^{3.11} \quad (5)$$

($R^2 = 0.46$, $N = 21$, $p = 7.3 \times 10^{-4}$). The statistical indices applied for the formulae were also obtained for Eq. (5). Note that this equation is not comparable with the rest of assessed formulae, since it is a regression equation derived from own data of the study reach. Although indices for Eq. (5) were not taken into account in the ranking of the formulae, they are shown at the bottom of Tables 5–7 in order to facilitate comparisons between the Ebro bed load model and the 10 different formulae that were selected.

7. Testing the formulae

7.1. Bed Material Division

Tables 5 and 6 show the statistical indices according to the Bed Material Division and considering the different sediment grain-size scenarios (i.e., subsurface and surface, respectively). In these tables, the value of each statistical index is ordered from the smallest to the largest discrepancy between the values for q_{sp} and q_{so}; this is a way of ranking the predictive power of each formula. It is important to note that we have included formulae that explicitly consider the presence of an armor layer (i.e., P–K–M and Bt) (Tables 5 and 6) despite these formulae directly specify the material (i.e., surface and/or subsurface) required to predict bed load discharge (see Section 4.3).

When we used subsurface grain size distribution in the BMD the overall best fit was provided by P–K–M, B, Y and the Rottner (1959) (hereafter R) formulae (Table 5). This can be seen in Figs. 4 and 6a in which these three formulae show less scatter than the others. The worst performing formulae were those of Meyer-Peter and Müller (1948) (hereafter MP–M), E–B and Wong and Parker (2006) (hereafter W–P); mainly due to their trend to overpredict. When the surface bed material was used in the BMD, there were smaller discrepancies between P–K–M and Y and the observed data (Table 6). However, Fig. 6b reveals that Y produced greater scatter for r than P–K–M (especially for the lower limit, since the Y formula predicted no bed load discharge (i.e., zero bed load) for 5 values (see Fig. 4)). The E–B formula performed well, although it showed a larger scatter of r between percentiles 25 and 75 (Fig. 6b). The worst performing formulae were B and S, mainly because they tended to underestimation (Figs. 4 and 6b).

Figs. 4, 6a and b illustrate an overall tendency to underestimate (e.g., median discrepancy ratio $r < 1$) when surface material is used; in contrast, overestimation occurs when subsurface material is used as a grain-size predictive variable (e.g., median discrepancy ratio $r > 1$). All the formulae (except P–K–M and Bt) that use subsurface material yielded an arithmetic mean of the median values of r (where the reciprocal value was used if the median value of $r < 1$) of 9.3, with a coefficient of variation of 125%. When surface material was used, the arithmetic mean of the median values of r (where the reciprocal value was used if the median value of $r < 1$) was 112 and the coefficient of variation was 126%. Underestimation using surface material is therefore, on average, one order of magnitude higher than overestimation using subsurface material. This pattern can mainly be attributed to the fact that surface material was too coarse to be theoretically entrained for most of the eight formulae. In similar way, the relative fine texture of the subsurface materials drives to overprediction. Fig. 4 illustrates the different proportion of zero bed load predictions when using surface and subsurface materials.

Finally, armoring was greater for BMI than for BMII (Table 1). This may explain the larger discrepancy between the predictions when surface and subsurface materials were alternatively used to feed the formulae under the BMI division (Fig. 4). In some cases this discrepancy was notably large since the surface material for BMI was too coarse for the flow to exceed the predicted entrainment threshold (which was based on the formulation, see Appendix A). This was evident, especially for equations S, B, W–P and A–W; none of these equations showed more than three values (for BMI surface material) that exceeded the entrainment condition value (Fig. 4).

7.2. Armor Layer Division

Table 7 shows the values of indices according to the Armor Layer Division. In this table, each of the statistical index values is

Table 5
Comparison of the predictive power of the formulae according to the Bed Material Division (BMD) and using the subsurface bed material to feed the formulae. Note that results are sorted from best to worst performance according to each index. In bold the formulae ranked in the first four positions according to the combined evaluation criteria (see criteria in Section 5).

Formula	r (0.5–2)[a] (%)	Formula	r (0.2–5)[b] (%)	Formula	r (0.1–10)[c] (%)	Formula	mr[d] (–)	Formula	mlr (–)	Formula	gr (–)	Formula	gwr (–)
P–K–M[e]	50	**B**	83	**B**	97	A–W	1.7	**P–K–M**	−0.04	**B**	2.4	**P–K–M**	2.60
B	47	**Y**	83	**P–K–M**	92	**P–K–M**	2.6	**B**	−0.09	**Y**	2.7	**R**	2.75
Y	44	**P–K–M**	78	**Y**	89	**B**	2.9	**R**	0.21	**P–K–M**	2.8	S	2.77
A–W	36	S	75	**R**	89	**R**	4.0	**Y**	0.30	S	3.7	**Y**	2.79
R	28	**R**	67	S	86	**Y**	7.1	A–W	−0.34	**R**	3.8	A–W	3.70
S	25	A–W	67	Bt	74	Bt	8.4	Bt	0.42	A–W	5.0	**B**	4.60
Bt[e]	9	Bt	30	A–W	72	S	20.2	S	0.52	Bt	6.9	W–P	10.39
W–P	0	W–P	14	W–P	28	W–P	98.7	W–P	1.27	W–P	18.7	E–B	12.59
E–B	0	E–B	8	E–B	28	E–B	152.5	E–B	1.34	E–B	21.7	Bt	28.16
MP–M	0	MP–M	3	MP–M	11	MP–M	237.3	MP–M	1.62	MP–M	41.9	MP–M	29.06
Eq. (5)[f]	53	Eq. (5)	86	Eq. (5)	94	Eq. (5)	6.5	Eq. (5)	0.20	Eq. (5)	2.5	Eq. (5)	2.95

[a] $0.5 < r < 2$, the average percentage of predicted bed load discharge not exceeding a factor of 2 in relation to the observed discharge.
[b] $0.2 < r < 5$, the average percentage of predicted bed load discharge not exceeding a factor of 5 in relation to the observed discharge.
[c] $0.1 < r < 10$, the average percentage of predicted bed load discharge not exceeding a factor of 10 in relation to the observed discharge.
[d] The values were ranked according to their proximity to $mr = 1$. Only for this purpose, the values in the range (0, 1) were recalculated as $1/mr$.
[e] Formula that directly specify the (surface and/or subsurface) material required to predict bed load discharge. Only values for whose formulae predicted broken armor condition were included (i.e., $N = 36$ in case of P–K–M, and $N = 23$ in Bt). See Section 4.3 for more details.
[f] Eq. (5) was not included in the formulae performance ranking, it is just presented as a reference.

ordered from small to large discrepancies between q_{sp} and q_{so}; this makes it possible to rank the predictive power of each formula.

P–K–M and Y show the best performance, followed by the W–P formula (Table 7). Fig. 6c shows that the P–K–M formula produced much less scatter than the other two equations. This may be due to the fact that P–K–M predictions only corresponded to data from the Broken Armor Layer (BAL) subgroup (see Section 4.3.); whereas predictions by the other two formulae experienced the negative impact of zero predictions in the Unbroken Armor Layer (UAL) subgroup (Fig. 5). Bt, B and A–W showed the lowest levels of predictive power.

Fig. 3b illustrates that the bed load rating curve for the BAL data subgroup plotted above the curves of the UAL and Reestablished Armor Layer (RAL), with higher values of q_s for the same value of Q, showing the effects of the armor break-up. BAL and RAL are the two closest subgroups in Fig. 3b, with an overlap for q_s between 0.5 and 1.50 N s^{-1} m^{-1}. In contrast to RAL, there are up to seven values of BAL for q_s > 1.50 N s^{-1} m^{-1}. However, this trend was not well predicted by most of the formulae that were studied. Fig. 5 indicates that frequently predicted q_s values for RAL plotted at the same level, or even higher level, than those of the BAL subgroup. This can mainly be attributed to the fact that the combined bed material of BMI applied for BAL condition is similar to the surface material of BMII (used under RAL conditions). In contrast, most of the predictions for the UAL subgroup were below those obtained for BAL and RAL (Fig. 5); most of the predictions for UAL yielded 0 (except for the E–B and Y formulae). This may have been related to the coarse size of the BMI surface bed-material (Table 1).

Overall, a larger deviation between predicted and measured bed load discharge was observed for low flow discharges near the observed threshold of mobility (e.g., Habersack and Laronne, 2002; Barry et al., 2004; Recking, 2010). This would be the case of the predictions from E–B and Y in relation to the lowest observed values for the UAL subgroup (Fig. 5). The fact that the UAL data were the ones with the largest proportion of q_{so} < 0.01N s^{-1} m^{-1} (Fig. 3b) helps to explain the poor performance of the formulae tested for this subgroup. This also explains why the global performances of most of the formulae were not appreciably better for the Armor Layer Division than for the Bed Material Division (fed by subsurface material). However, for the ALD condition and all the formulae, the arithmetic mean of the median values of r (where the reciprocal value was used if the median value of r < 1) was 7.4

Table 6
Comparison of the predictive power of the formulae according to the Bed Material Division (BMD) and using the surface bed material to feed the formulae. Note that results are sorted from best to worst performance according to each index. In bold the formulae ranked in the first three positions according to the combined evaluation criteria (see criteria in Section 5).

Formula	r (0.5–2)[a] (%)	Formula	r (0.2–5)[b] (%)	Formula	r (0.1–10)[c] (%)	Formula	mr[d] (–)	Formula	mlr (–)	Formula	gr (–)	Formula	gwr (–)
P–K–M[e]	50	**P–K–M**	78	**P–K–M**	92	**P–K–M**	2.60	**P–K–M**	−0.04	**P–K–M**	2.8	**P–K–M**	3
Y	28	**Y**	64	**E–B**	78	**Y**	2.80	**E–B**	0.17	**E–B**	6.1	**Y**	6
R	19	**E–B**	42	Bt	74	W–P	2.90	**Y**	−0.22	**Y**	6.5	**E–B**	10
S	14	R	39	**Y**	69	R	0.31	Bt	0.42	Bt	6.9	Bt	28
A–W	14	Bt	30	W–P	44	**E–B**	5.70	MP–M	−0.73	R	44.8	R	149
W–P	11	W–P	25	R	42	A–W	0.15	W–P	−1.19	W–P	59.3	MP–M	162
Bt[e]	9	S	19	MP–M	28	S	0.12	R	−1.61	MP–M	61.7	A–W	862
E–B	6	A–W	19	A–W	25	Bt	8.40	A–W	−2.04	A–W	110.1	W–P	3090
MP–M	3	B	14	B	25	MP–M	9.10	B	−2.13	B	135.6	B	4769
B	3	MP–M	11	S	22	B	0.07	S	−2.21	S	161.8	S	6348
Eq. (5)[f]	53	Eq. (5)	86	Eq. (5)	94	Eq. (5)	6.54	Eq. (5)	0.20	Eq. (5)	2.5	Eq. (5)	3

[a] 0.5 < r < 2, the average percentage of predicted bed load discharge not exceeding a factor of 2 in relation to the observed discharge.
[b] 0.2 < r < 5, the average percentage of predicted bed load discharge not exceeding a factor of 5 in relation to the observed discharge.
[c] 0.1 < r < 10, the average percentage of predicted bed load discharge not exceeding a factor of 10 in relation to the observed discharge.
[d] The values were ranked according to their proximity to mr = 1. Only for this purpose, the values in the range (0, 1) were recalculated as 1/mr.
[e] Formula that directly specify the (surface and/or subsurface) material required to predict bed load discharge. Only values for whose formulae predicted broken armor condition were included (i.e., N = 36 in case of P–K–M, and N = 23 in Bt). See Section 4.3 for more details.
[f] Eq. (5) was not included in the formulae performance ranking, it is just presented as a reference.

Table 7
Comparison of the predictive power of the formulae according to the Armor Layer Division (ALD). Note that results are sorted from best to worst performance according to each index. In bold the formulae ranked in the first two positions according to the combined evaluation criteria (see criteria in Section 5).

Formula	r (0.5–2)[a] (%)	Formula	r (0.2–5)[b] (%)	Formula	r (0.1–10)[c] (%)	Formula	mr[d] (–)	Formula	mlr (–)	Formula	gr (–)	Formula	gwr (–)
P–K–M[e]	47	**P–K–M**	67	**P–K–M**	93	**P–K–M**	0.90	MP–M	−0.01	**P–K–M**	3.1	**Y**	2.5
Y	34	**Y**	66	**Y**	78	R	0.50	**Y**	0.17	**Y**	5.7	E–B	3.0
W–P	24	E–B	54	E–B	76	W–P	2.96	**P–K–M**	−0.33	E–B	7.5	**P–K–M**	6.6
S	20	R	51	W–P	71	S	0.27	W–P	−0.68	Bt	12.2	MP–M	7.9
A–W	20	W–P	44	R	61	A–W	0.24	E–B	0.87	MP–M	16.2	W–P	8.9
E–B	17	S	39	MP–M	56	B	0.11	Bt	−1.09	W–P	18.4	R	10.2
R	17	MP–M	32	S	51	MP–M	9.21	R	−1.25	R	21.1	S	24.1
MP–M	10	A–W	32	A–W	44	Bt	0.09	S	−1.86	B	71.8	B	57.3
B	5	B	20	B	42	E–B	100.80	B	−1.86	S	75.0	A–W	63.9
Bt[e]	0	Bt	0	Bt	25	**Y**	209.30	A–W	−2.09	A–W	126.9	Bt	>10^6
Eq. (5)[f]	41	Eq. (5)	76	Eq. (5)	85	Eq. (5)	388.90	Eq. (5)	0.50	Eq. (5)	5.3	Eq. (5)	2.8

[a] 0.5 < r < 2, the average percentage of predicted bed load discharge not exceeding a factor of 2 in relation to the observed discharge.
[b] 0.2 < r < 5, the average percentage of predicted bed load discharge not exceeding a factor of 5 in relation to the observed discharge.
[c] 0.1 < r < 10, the average percentage of predicted bed load discharge not exceeding a factor of 10 in relation to the observed discharge.
[d] The values were ranked according to their proximity to mr = 1. Only for this purpose, the values in the range (0, 1) were recalculated as 1/mr.
[e] Formula that directly specify the (surface and/or subsurface) material required to predict bed load discharge. Only data for the BAL subset were included (i.e., N = 15 in case of P–K–M, and N = 4 in Bt). See Section 4.3 for more details.
[f] Eq. (5) was not included in the formulae performance ranking, it is just presented as a reference.

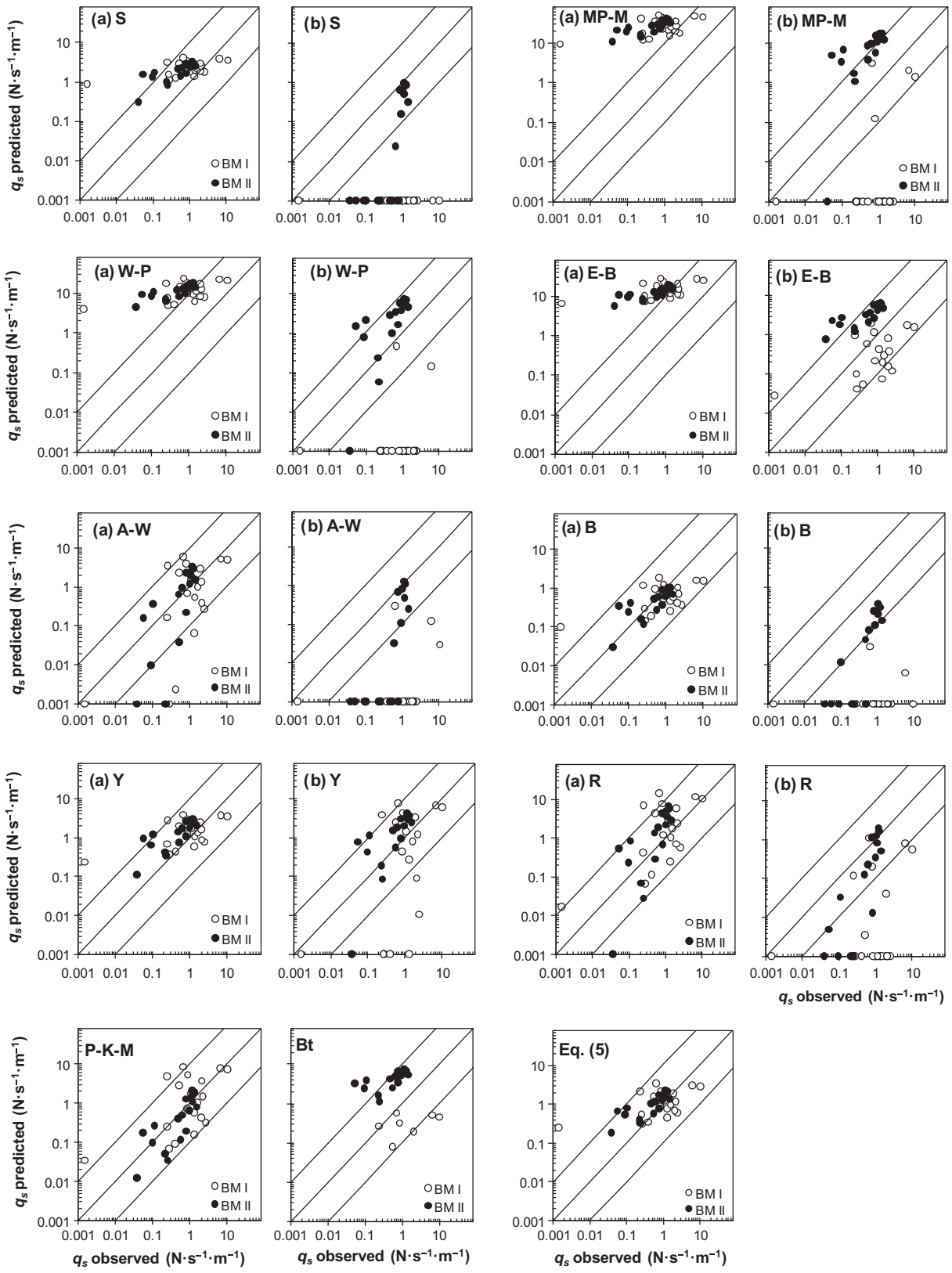

Fig. 4. Predicted unit bed load discharge using selected formulas plotted against observed rates according to the Bed Material Division (BMD) and using (a) subsurface bed material and (b) surface bed material. Note that the P–K–M and Bt formulae directly specify the (surface and/or subsurface) material required to predict bed load discharge. Lines parallel to the line of perfect equality ($r = 1$) correspond to $r = 0.1$ and $r = 10$. Values plotted on the x axis correspond to bed load zero predictions.

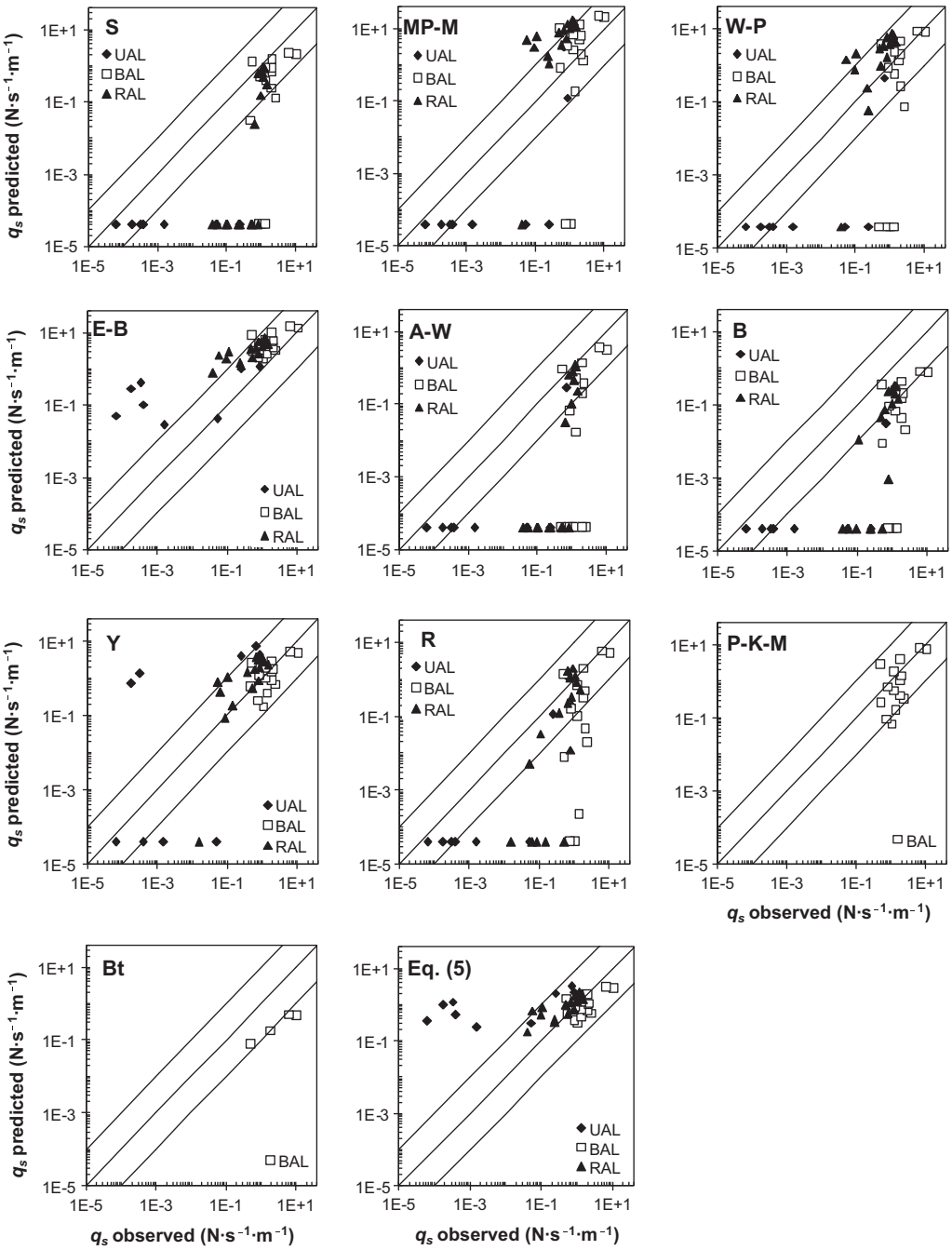

Fig. 5. Predicted unit bed load discharge by evaluated formulas plotted against observed rates according to the Armor Layer Division (ALD); i.e., UAL: Unbroken Armor Layer, BAL: Broken Armor Layer, and RAL: reestablished armor layer. Lines parallel to the line of perfect equality ($r = 1$) correspond to $r = 0.1$ and $r = 10$. Values plotted parallel to the x axis correspond to bed load zero predictions.

and the coefficient of variation was 88% (7.6 and 91%, respectively, if P–K–M and Bt are excluded). These are more significant values that the obtained for the BMD condition (see Section 7.1). This fact indicates, in general terms, that considering the armor condition improves the explanatory power of the bed load formulae.

8. Discussion

The results show that the predictive power of the tested formulae is relatively low, although on the range observed in the literature. The low accuracy of the formulae is known by every engineering standard, where commonly a much higher accuracy is required. Overall, including the 10 formulae and all the scenario divisions, the average percentages of predicted bed load discharge (q_{sp}) not exceeding a factor of 2 ($0.5 < r < 2$), 5 ($0.2 < r < 5$) and 10 ($0.1 < r < 10$) in relation to the observed discharge (q_{so}) were 19%, 41% and 57%, respectively. Although this degree of discrepancy may seem rather large, it is not unreasonable in comparison to previous studies that explored the performance of bed load transport formulae in gravel bedded rivers (see Table 8 for comparison with a selection of recent studies). Worth to point out that our results and consequent conclusions may be sensitive to the available sampling period (2 years) and the small sample size (one river). A longer sampling period might weight the distribution of observed transport rates differently than those observed over the current 2-year period, potentially changing equation performance.

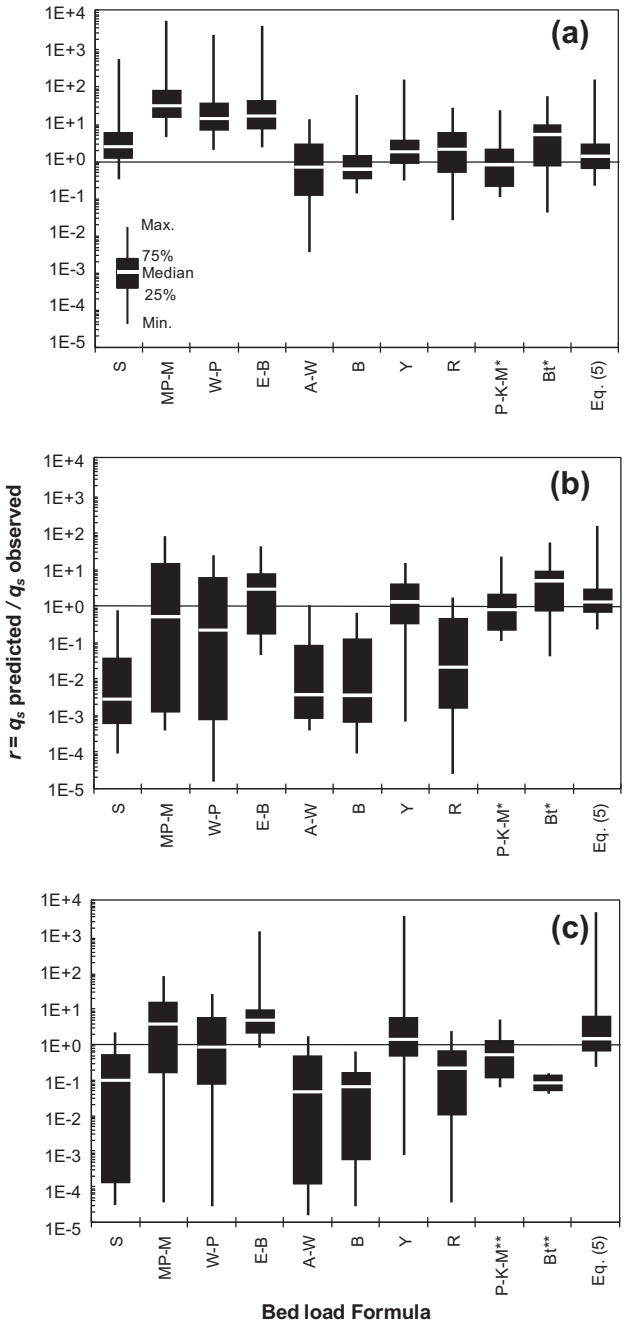

Fig. 6. Box plots of the distribution of the ratio between predicted and observed unit bed load discharge according to data sets: (a) Bed Material Division (BMD) data fed by subsurface bed material; (b) Bed Material Division (BMD) data fed by surface bed material; and (c) Armor Layer Division (ALD). Note that (∗) indicates that the P–K–M and Bt formulae directly specify the (surface and/or subsurface) material required to predict bed load discharge; likewise formulae with (∗∗) indicates that only BAL data was used (see Section 4.3 for more details).

However, the advantage of the sampled years is that these represent significantly different bed conditions; more stable because the well-developed armor layer and more mobile because the effects of the break-up of the armor layer. These conditions are also sensitive to bed load performance as is analyzed in this study. Equation performance also varies between rivers (e.g., Barry et al., 2008) and that results might differ if the analyses had been conducted across a range of rivers.

The P–K–M (Parker et al., 1982) and Y (Yang, 1984) formulae presented the better levels of agreement with observed bed load discharges. Overall, these formulae were always ranked in the first positions according to the combined evaluation criteria. The Y formula maintained a high predictive power (i.e., relatively good performance) even when the bed texture used for its formulation changed from subsurface to surface material (in the Bed Material Division, BMD). This is related to the relatively low sensitivity of the formula to the bed material in question, which is discussed later in this section. The P–K–M formula, in contrast, does not take into account the bed material criteria; the formula is run when it is considered that the driving force exceeds the armor break up condition. The performance of the majority of the formulae declined when surface material is used in the BMD. Also was observed the variability in ranking of formulae performance once the bed texture had changed. For instance, B formulae (Bagnold, 1980), E–B (Einstein–Brown, in Brown, 1950), W–P (Wong and Parker, 2006) appear either near the top or near the bottom of the performance ranking depending on the bed texture used in their calculations.

In global terms, although the results show substantial differences in equation performance, no evident and categorical relationships were found between the predictive power of the formulae and their theoretical approach. However, in this study, the formulae that performed best maintained their accuracy much more constantly over the whole range of discharges than formulae with a low level of performance and whose accuracy was highly variable. This pattern is observed in Fig. 4 by comparing the performance of the P–K–M, B and Y formulae with those of the E–B and MP–M formulae. More specifically, the latter group shows how overestimation increases as bed load discharge decreases. Equation performance may vary in relation to site characteristics, sampling conditions and representativeness. For instance, Barry et al. (2008) attributed part of this discrepancy to differences in the frequency of the discharges used for assessing the performance of these equations (e.g., bankfull discharge vs. low flows).

Only 2 of the 10 formulae that were tested explicitly include the effects of river bed armoring in their theoretical principles: P–K–M and Bt (see Appendix A and Table 2). The Bt formula only quantifies bed load discharge once the armor has been broken, while the P–K–M formula considers equal mobility once the armor has been broken (see Appendix A for criteria). As a result, only the predictions that exceeded the threshold above which the armor layer broke were considered when these two formulae were evaluated according to the Bed Material Division. In turn, only the predictions within the Break Armor Layer (BAL) group were considered when these formulae were evaluated according to the Armor Layer Division. Taking these considerations into account, the discrepancy between predicted and observed bed load discharges was smaller in the case of the P–K–M formula than in that of Bt (Fig. 6). P–K–M formula that presented one of the best levels of agreement with the observed bed load discharges, as discussed above. In contrast, the Bt formula was ranked within the five worst formulae in terms of prediction. In this case, the relatively poor performance could be attributed to the overestimation of the threshold above which the armor layer breaks up.

As already pointed out, the Yang formula produced one of the best performances, irrespective of the division that was considered. However, it is worth noting that in some cases the Y formula predicts an increase in bed load rates associated with an increase in sediment grain size (see Figs. 4 and 5); this observation contradicts the physical phenomena that were modeled. A similar finding was reported by Chang (1988) and Julien (1998); for the sand bed load formula by the same author (i.e., Yang, 1973) a slight increase in sediment transport capacity was detected with grain size for coarse sands. The Y formula is not as sensitive to grain-size as other formulae, and, therefore, is less likely to produce wide variations in calculated sediment transport (USACE, 1989). Similarly, the Y

Table 8
Performance of the formulae compared with a selection of recent studies in gravel bed streams.

Reference	N^a	r (0.5–2)[b] (%)	r (0.2–5)[c] (%)	r (0.1–10)[d] (%)	Observations
Habersack and Laronne (2002)	13	36	–	–	Alpine gravel bed river
Martin (2003)	4	19	44	75	Annual gravel transport in 10 reaches of a gravel bed river
Martin and Ham (2005)	3	11	25	47	Average annual gravel transport in 13 reaches of a gravel bed river
Duan et al. (2006)	3	–	–	57	Low flow in two reaches of a desert gravel bed stream
Recking (2010)	4	13	27	34	6319 data from 84 reaches of sand and gravel bed rivers
This study (River Ebro)	10	19	41	57	Regulated river experiencing cycles of armoring

[a] Number of formulas involved in the study.
[b] $0.5 < r < 2$, the average percentage of predicted bed load discharge not exceeding a factor of 2 in relation to the observed discharge.
[c] $0.2 < r < 5$, the average percentage of predicted bed load discharge not exceeding a factor of 5 in relation to the observed discharge.
[d] $0.1 < r < 10$, the average percentage of predicted bed load discharge not exceeding a factor of 10 in relation to the observed discharge.

formula performed consistently well even when surface material was substituted by subsurface material in the BMD analysis; this contrasted with the observed decrease in predictive power shown by most of the other equations that were studied.

The overestimation by the MP–M formula observed in this study could have been due to the adoption of the plane-bed hypothesis (i.e., $k/k' = 1$ and therefore no form of drag correction); although several studies have already detected that it overpredicts bed load transport under plane-bed conditions (i.e., in the absence of a form drag correction) (Wong and Parker, 2006). It should be noted that the W–P formula was developed as an improved version of the MP–M equation using part of the original database (Table 2). The results obtained show significantly smaller estimates than those produced by the original formula under plane-bed conditions (with differences of a factor of 2.0–2.5) (Wong and Parker, 2006). Our results indicate that the MP–M formula (with no form drag correction) predicts higher rates that those obtained by the W–P equation; the values differed by a factor of between 2 and 3 once the entrainment threshold had been exceeded.

The best predictions of the Ebro bed load rating curve (equation 5) were similar to those of the best performing formulae. The best predictions were obtained for the BMD using surface material; in this case, our model produced the best performance according to five of the seven statistical indices (Table 6). In contrast, its performance for ALD analysis was not significantly better than that of the other 10 equations (Table 7). This may be attributed to the large discrepancy associated with the Unbroken Armor Layer condition (see Fig. 3b). Although the regression expressed in Eq. (5) was statistically significant, it only explained 46% of the bed load variability. Overall, we can conclude that the performance of Eq. (5) was not definitely better than the best ranked models analyzed in this study. In the case of the Ebro, the predictive power of the general bed load model was clearly limited because the only independent variable was flow discharge; as a result, the equation cannot fully explain phenomena such as the temporal variability of bed grain-size or the cycle according to which armor layer was broken up and re-established during the study period.

Our work principally aimed at assessing the predictive power of a series of bed load formulae tested against bed load transport rates obtained for a large regulated gravel bed river. We do not intend at any kind of formulae calibration or process-based reassessment; but to give practitioners a guide of formulae performance applicable to large regulated rivers in which, generally, field data is scarce and riverbed dynamics difficult to observe. Results provide insights into variability of real processes and model performance, according to bed material characteristics and structure (Fig. 7). Although, on average, bed surface material provides best model performance, it is worth to notice that models predicting the lowest transport rates (lower envelopes in Fig. 7) best

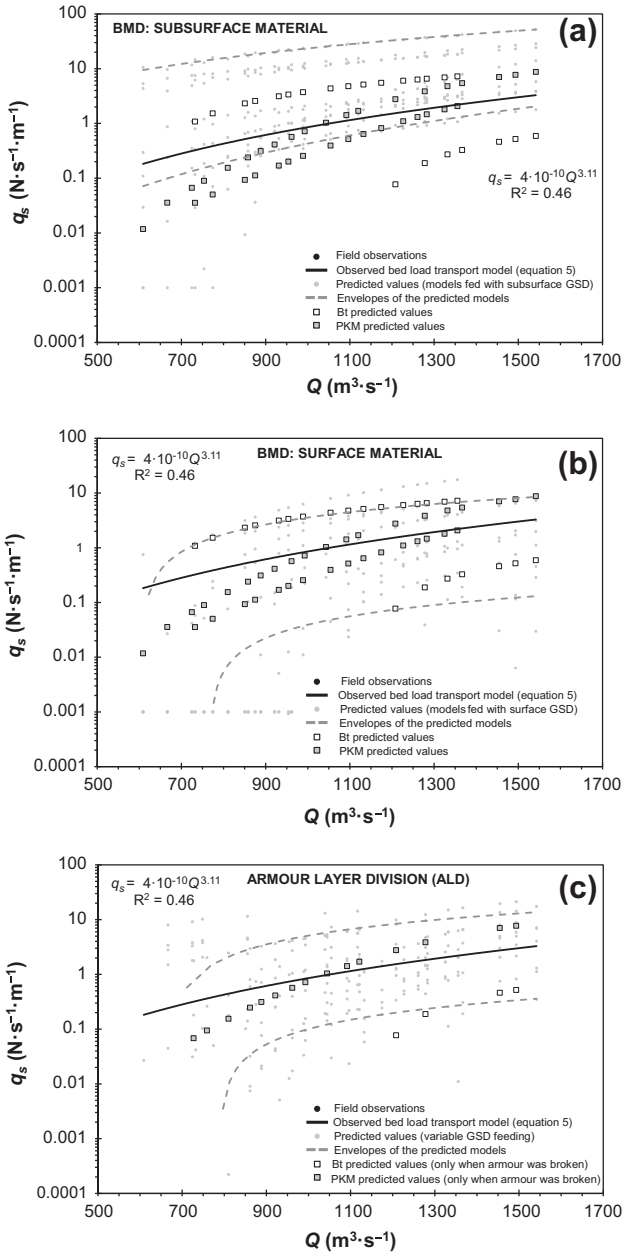

Fig. 7. Summary of model performance for the different Bed Material Division (BMI and BMII) and armoring conditions (ALD). The observed bed load average model (Eq. (5)) is highlighted for reference.

resembles the observed Ebro model (Eq. (5)), when they are fed with subsurface material (Fig. 7a). This fact is relevant for practitioners managing supply limited systems (i.e., regulated rivers) since these conservative models may support the design of actions aiming at restoring geomorphic processes, but minimizing negative effects such as bed incision; furthermore, considering the armor condition improves the explanatory power of the bed load formulae.

9. Conclusions

This paper aims to evaluate the predictive power of 10 bed load formulae tested against bed load transport rates obtained in a large regulated river (River Ebro) that is subject to cycles of break-up and reestablishment of its armor layer. The average percentages of predicted bed load discharge that did not exceed factors of 2 ($0.5 < r < 2$) and 10 ($0.1 < r < 10$) in relation to the observed discharge were 19% and 57%. This degree of discrepancy is relatively large but it is on the range observed in the literature. The P–K–M and Y formulae presented the better levels of agreement with observed bed load discharges. The formulae that performed best maintained their accuracy much more constantly over the whole range of discharges. The performance of the majority of the formulae declined when surface material is used in the BMD. It has been found that considering the armor condition improve the explanatory power of the bed load formulae. The discrepancy between predicted and observed bed load discharges was smaller in the case of the P–K–M formula than in that of Bt (the only 2 of the 10 formulae that explicitly include the effects of river bed armoring in their development). The bed load rating curve for the lower Ebro showed a similar degree of agreement to the best-performing formulae.

Acknowledgements

This research was carried out within the framework of the Research Projects REN2001-0840-C02-01/HID, CGL2005-06989-C02-02/HID, CGL2006-11679-C02-01/HID, CGL2009-09770 (subprograma BTE), and SCARCE Consolider Ingenio 2010 CSD2009-00065, all funded by the Spanish Ministry of Science and Technology. The second author has benefit from a Juan de la Cierva Fellowship (JCI-2008-2910) funded by the Spanish Ministry of Science and Innovation and a Ramon y Cajal Fellowship (RYC-2010-06264) funded by the Spanish Ministry of Science and Innovation. Hydrological data were supplied by the Ebro Water Authorities. The Móra d'Ebre Town Council provided logistical support during fieldwork. Albert Rovira assisted during fieldwork and labwork. Comments by Jonathan B. Laronne, John Buffington and anonymous reviewers were extremely helpful in improving the manuscript.

Appendix A. Bed load transport formulae

A.1. Schoklitsch (1950)

$$q_{sv} = 2.5(\gamma_s/\gamma)^{-1}S^{3/2}(q - q_c) \tag{A1}$$

$$q_c = 0.26((\gamma_s/\gamma) - 1)^{5/3}D_{40}^{3/2}S^{-7/6} \text{ when } D_{40} \geqslant 0.006 \text{ m} \tag{A2}$$

where q_{sv} is the bed load discharge in volume per unit width ($m^3\ s^{-1}\ m^{-1}$), γ_s is the specific weight of sediment, γ is the specific weight of water, q is the water discharge per unit width ($m^3\ s^{-1}\ m^{-1}$), q_c is the critical water discharge per unit width ($m^3\ s^{-1}\ m^{-1}$), S is the channel slope ($m\ m^{-1}$), and D_{40} is the particle size for which 40% of the bed material is finer (m).

A.2. Meyer-Peter and Müller (1948)

$$\left[\frac{q_s(\gamma_s - \gamma)}{\gamma_s}\right]^{2/3}\left[\frac{\gamma}{g}\right]^{1/3}\frac{0.25}{(\gamma_s - \gamma)D_m} = \frac{(k/k')^{3/2}\gamma RS}{(\gamma_s - \gamma)D_m} - 0.047 \tag{A3}$$

where q_s is the bed load discharge in weight per unit width, g is the gravitational acceleration, k is the Manning coefficient of roughness associated with skin friction only, k' is the Manning coefficient of total roughness ($k/k' = 1$, in this study), R is the hydraulic radius, and D_m is the arithmetic mean diameter.

A.3. Wong and Parker (2006)

$$q_{sv} = q_*\sqrt{((\gamma_s/\gamma) - 1)gD_m}D_m \tag{A4}$$

$$q_* = 4.93(\tau_* - 0.0470)^{1.60} \tag{A5}$$

$$\tau_* = \frac{\gamma RS}{(\gamma_s - \gamma)D_m} \tag{A6}$$

where q_{sv} is the bed load discharge in volume per unit width, q_* is the dimensionless volumetric bed load transport rate per unit width, and τ_* is the Shields number.

A.4. Einstein–Brown, Brown (1950)

$$q_{sv} = q_*F_1\sqrt{((\gamma_s/\gamma) - 1)gD_{50}^3} \tag{A7}$$

$$F_1 = \left[\frac{2}{3} + \frac{36\nu^2}{g((\gamma_s - \gamma)/\gamma)D_{50}^3}\right]^{0.5} - \left[\frac{36\nu^2}{g((\gamma_s - \gamma)/\gamma)D_{50}^3}\right]^{0.5} \tag{A8}$$

$$q_* = 2.15\exp(-0.391/\tau_*) \quad \text{when} \quad \tau_* < 0.09 \tag{A9a}$$

$$q_* = 40\tau_*^3 \quad \text{when} \quad \tau_* > 0.09 \tag{A9b}$$

$$\tau_* = \frac{\gamma RS}{(\gamma_s - \gamma)D_{50}} \tag{A10}$$

where q_{sv} is the bed load discharge in volume per unit width, q_* is the dimensionless volumetric bed load transport rate per unit width, F_1 is the parameter of fall velocity, ν is the kinematic viscosity of water, and D_{50} is the median particle diameter.

A.5. Ackers and White (1973), Ackers (1993)

$$q_{stv} = qG_{gr}\frac{D_{35}}{y}\left[\frac{V}{U_*}\right]^n \tag{A11}$$

$$G_{gr} = C((F_{gr}/A_{gr}) - 1)^m \tag{A12}$$

$$U_* = \sqrt{gRS} \tag{A13}$$

$$F_{gr} = \frac{U_*^n}{\sqrt{gD_{35}((\gamma_s/\gamma) - 1)}}\left[\frac{V}{\sqrt{32}\log(10y/D_{35})}\right]^{1-n} \tag{A14}$$

$$D_{gr} = D_{35}\left[\frac{g((\gamma_s/\gamma) - 1)}{\nu^2}\right]^{1/3} \tag{A15}$$

for $D_{gr} > 60$

$$n = 0.0; \quad m = 1.78; \quad A_{gr} = 0.17; \quad C = 0.025 \tag{A16}$$

for $1 < D_{gr} < 60$

$$\log C = 2.79\log D_{gr} - 0.98(\log D_{gr})^2 - 3.46; \quad n = 1 - 0.56\log D_{gr} \tag{A17}$$

$$m = 1.67 + \frac{6.83}{D_{gr}}; \quad A_{gr} = 0.14 + \frac{0.23}{\sqrt{D_{gr}}} \tag{A18}$$

where q_{stv} is the total bed-material load in volume per unit width, y is the mean flow depth, V is the mean flow velocity, U_* is the shear velocity, G_{gr} is the dimensionless transport rate; C is a coefficient, F_{gr} is the sediment mobilization parameter, A_{gr} is the threshold of mobility, D_{gr} is the non-dimensional sediment size, n is a transition parameter varying from 1.0 for fine material to 0 for coarse material, and m is the exponent of the transport formula.

A.6. Bagnold (1980)

$$q_{sm} = \frac{\rho_s}{\rho_s - \rho} q_{sr} \left[\frac{\omega - \omega_c}{(\omega - \omega_c)_r}\right]^{3/2} \left[\frac{y}{y_r}\right]^{-2/3} \left[\frac{D_{50}}{D_{50r}}\right]^{-1/2} \tag{A19}$$

$$\omega = \rho y S V \tag{A20}$$

$$\omega_c = 5.75((\rho_s - \rho)D_{50}0.04)^{3/2}(g/\rho)^{1/2}\log(12y/D_{50}) \tag{A21}$$

or

$$\omega_c \approx 290 D_{50}^{3/2}\log(12y/D_{50}) \tag{A22}$$

$$q_{sr} = 0.1 \text{ kg s}^{-1}\text{ m}^{-1}; \quad (\omega - \omega_c)_r = 0.5 \text{ kg s}^{-1}\text{ m}^{-1}; \quad y_r = 0.1 \text{ m}; D_{50r} = 0.0011 \text{ m} \tag{A23}$$

where q_{sm} is the bed load discharge in mass per unit width (kg s^{-1} m^{-1}), ρ_s is the density of sediment (kg m^{-3}), ρ is the density of water (kg m^{-3}), ω is the stream power per unit bed area (in mass units, kg s^{-1} m^{-1}), ω_c is the critical unit stream power at the beginning of movement (kg s^{-1} m^{-1}), q_{sr} is the reference value of q_{sm} (kg s^{-1} m^{-1}), $(\omega - \omega_c)_r$ is the reference value of excess stream power (kg s^{-1} m^{-1}); y_r is the reference value of y (m), and D_{50r} is the reference value of D_{50} (m). Note that in this study we have modified this equation by (1) using D_{50} instead of the characteristic particle size in the original formulation, (2) using a fixed grain-size rather than an event-based, and (3) using a different grain-size distribution according to data division: surface, subsurface or combined, rather than the bed load grain-size.

A.7. Yang (1984)

$$q_{stw} = 10^{-3} \cdot y \cdot V \cdot C \tag{A24}$$

$$C \approx C_s \tag{A25}$$

$$\log C_s = 6.681 - 0.633\log\left[\frac{w_s D_{50}}{\nu}\right] - 4.816\log\left[\frac{U_*}{w_s}\right] + \left\{2.784 - 0.305\log\left[\frac{w_s D_{50}}{\nu}\right] - 0.282\log\left[\frac{U_*}{w_s}\right]\right\}\log\left[\frac{VS}{w_s} - \frac{V_c S}{w_s}\right] \tag{A26}$$

$$U_* = \sqrt{gRS} \tag{A27}$$

$$w_s = F_1(g((\gamma_s - \gamma)/\gamma)D_{50})^{0.5} \tag{A28}$$

$$F_1 = \left[\frac{2}{3} + \frac{36\nu^2}{g((\gamma_s - \gamma)/\gamma)D_{50}^3}\right]^{0.5} - \left[\frac{36\nu^2}{g((\gamma_s - \gamma)/\gamma)D_{50}^3}\right]^{0.5} \tag{A29}$$

$$\text{for} \quad 1.2 < \frac{U_* y}{w_s} < 70; \quad \frac{V_c}{w_s} = \frac{2.5}{\log(U_* y/\nu)} + 0.66 \tag{A30}$$

$$\text{for} \quad \frac{U_* y}{w_s} \geqslant 70; \quad \frac{V_c}{w_s} = 2.05 \tag{A31}$$

where q_{stw} is the total bed-material load discharge in weight per unit width (kp s^{-1} m^{-1}), q is the water discharge per unit width (m^3 s^{-1} m^{-1}), C is the total bed-material concentration in mg l^{-1}, C_s is the total bed-material concentration in ppm by weight, V_c is the mean velocity at incipient sediment motion, w_s is the fall velocity of sediment, and F_1 is the parameter of fall velocity.

A.8. Rottner (1959)

$$q_s = \gamma_s\sqrt{g\left[\frac{\gamma_s - \gamma}{\gamma}\right]D_{50}^3}\left\{\left[\frac{2}{3}\left[\frac{D_{50}}{y}\right]^{2/3} + 0.14\right]\frac{V}{\sqrt{g\left[\frac{\gamma_s - \gamma}{\gamma}\right]D_{50}}} - 0.778\left[\frac{D_{50}}{y}\right]^{2/3}\right\}^3 \tag{A32}$$

where q_s is the bed load discharge in weight per unit width.

A.9. Parker et al. (1982)

$$q_{sv} = W^*(yS)^{1.5}g^{0.5}((\gamma_s/\gamma) - 1)^{-1} \tag{A33}$$

$$\text{for} \quad 0.95 < \phi_{50} < 1.65; \quad W^* = 0.0025\exp(14.2(\phi_{50} - 1) - 9.28(\phi_{50} - 1)^2) \tag{A34}$$

$$\text{for} \quad \phi_{50} > 1.65; \quad W^* = 11.2(1 - (0.822/\phi_{50}))^{4.5} \tag{A35}$$

$$\phi_{50} = \tau^*_{50}/\tau^*_{r50} \tag{A36}$$

$$\tau^*_{50} = \frac{\gamma y S}{(\gamma_s - \gamma)D_{50s}}; \quad \tau^*_{r50} = 0.0876 \tag{A37}$$

where q_{sv} is the bed load in volume per unit width, W^* is the dimensionless bed load, D_{50s} is the median diameter of subsurface material, τ^*_{50} is the Shields stress for D_{50s}, τ^*_{r50} is the reference value of τ^*_{50}, and ϕ_{50} is the excess Shields stress.

A.10. Bathurst (2007)

$$q_{sm} = a\rho(q - q_{c_2}) \tag{A38}$$

$$a = 29.2S^{1.5}(D_{50}/D_{50s})^{-3.30} \tag{A39}$$

$$q_{c2} = 0.5(0.0513g^{0.5}D_{50}^{1.5}S^{-1.20} + 0.0133g^{0.5}D_{84}^{1.5}S^{-1.23}) \tag{A40}$$

where q_{sm} is the bed load discharge in mass per unit width (kg s^{-1} m^{-1}), q is the water discharge per unit width (m^3 s^{-1} m^{-1}), q_{c_2} is the threshold or critical water discharge per unit width for transport of material as the armor layer breaks up (m^3 s^{-1} m^{-1}), a is a dimensionless coefficient that represent the rate of change of bed load discharge with water mass discharge, ρ is the water density (kg m^{-3}), D_{50s} is the median diameter of subsurface material (m), D_{84} is the particle size of percentile 84 of surface layer material (m), g is the gravitational acceleration (m s^{-2}), and S is the channel slope (m m^{-1}).

References

Ackers, P., 1993. Sediment transport in open channels: Ackers and White update. Proc. Inst. Civil Eng. Water Marit. Energy 101, 247–249.

Ackers, P., White, W.R., 1973. Sediment transport: new approach and analysis. J. Hydraul. Div. 99 (11), 2041–2060.

Andrews, E.D., 1981. Measurement and computation of bed material discharge in a shallow sand-bed stream, Muddy Creek, Wyoming. Water Resour. Res. 17, 131–141.

Bagnold, R.A., 1980. An empirical correlation of bed load transport rates in flumes and natural rivers. Proc. Roy. Soc. Lond. Ser. A 372, 453–473.

Barry, J.J., Buffington, J.M., King, J.G., 2004. A general power equation for predicting bed load transport rates in gravel bed rivers. Water Resour. Res. 40, W10401. http://dx.doi.org/10.1029/2004WR003190.

Barry, J.J., Buffington, J.M., King, J.G., 2007. Correction to "A general power equation for predicting bed load transport rates in gravel bed rivers". Water Resour. Res. 43, W08702. http://dx.doi.org/10.1029/2007WR006103.

Barry, J.J., Buffington, J.M., Goodwin, P.G., King, J.G., Emmett, W.W., 2008. Performance of bed-load transport equations relative to geomorphic significance: predicting effective discharge and its transport rate. J. Hydraul. Eng. 134 (5), 601–615.

Batalla, R.J., 1997. Evaluating bed-material transport equations from field measurements in a sandy gravel-bed river. Earth Surf. Process. Land. 21, 121–130.

Batalla, R.J., Vericat, D., 2009. Hydrological and sediment transport dynamics of flushing flows: implications for management in large Mediterranean rivers. River Res. Appl. 25, 297–314.

Batalla, R.J., Gomez, C.M., Kondolf, G.M., 2004. Reservoir-induced hydrological changes in the Ebro River basin (Northeastern Spain). J. Hydrol. 290 (1–2), 117–136.

Bathurst, J.C., 2007. Effect of coarse surface layer on bed-load transport. J. Hydraul. Eng. 133 (11), 1192–1205.

Brown, C.B., 1950. Sediment transportation. In: Rouse, H. (Ed.), Engineering hydraulics. Wiley, New York, pp. 769–857.

Carson, M.A., Griffith, G.S., 1987. Bed load transport in gravel channels. J. Hydrol. (NZ) 26 (1), 1–151.

Casey, H.J., 1935. Über geschiebebewegung, Mitteilungen der Preussischen Versuchsanstalt. für Wasserbau und Schiffbau. 19, 86 pp.

Chang, Y.L., 1939. Laboratory investigation of flume traction and transportation. Trans. Am. Soc. Civil Eng. 104, 1246–1284.

Chang, H.H., 1988. Fluvial Processes in River Engineering. Wiley, New York.

Chang, H.H., 1994. Selection of gravel-transport formula for stream modeling. J. Hydraul. Eng. 120 (5), 646–651.

Church, M., McLean, D.G., Wolcott, J.F., 1987. River bed gravels: sampling and analysis. In: Thorne, C.R., Barthurst, J.C., Hey, R.D. (Eds.), Sediment Transport in Gravel-bed Rivers. John Wiley and Sons, Chichester, UK, pp. 43–88.

Dietrich, W.E., Kirchner, J.W., Ikeda, H., Iseya, F., 1989. Sediment supply and the development of the coarse surface layer in gravel-bedded rivers. Nature 340, 215–217.

Di Cristo, C., Iervolino, M., Vacca, A., 2006. Linear stability analysis of a 1-D model with dynamical description of bed-load transport. J. Hydraul. Res. 44 (4), 480–487.

Duan, J.G., Chen, L., Scott, S., 2006. Application of surface-based bed load transport equations to a desert gravel-bed stream. J. Hydraul. Res. 44 (5), 624–630.

Ferguson, R.I., 2003. The missing dimension: effects of lateral variation on 1-D calculations of fluvial bedload transport. Geomorphology 56, 1–14.

Fripp, J.B., Diplas, P., 1993. Surface sampling in gravel streams. J. Hydraul. Eng. 119 (4), 473–490.

Gilbert, G.K., 1914. The transportation of débris by running water. U.S. Geological Survey Professional Paper 86, 263 pp.

Gomez, B., 2006. The potential rate of bed-load transport. PNAS 103 (46), 17170–17173.

Gomez, B., Church, M., 1989. Assessment of bed load sediment transport formulae for gravel bed rivers. Water Resour. Res. 25 (6), 1161–1186.

Greco, M., Iervolino, M., Leopardi, A., Vacca, A., 2012. A two-phase model for fast geomorphic shallow flows. Int. J. Sediment. Res. 27 (4), 409–425.

Habersack, H., Laronne, J.B., 2002. Evaluation and improvement of bed load discharge formulas based on Helley–Smith sampling in an Alpine gravel bed river. J. Hydraul. Eng. 128 (5), 484–499.

Hamamori, A., 1962. A Theoretical Investigation on the Fluctuations of Bed Load Transport. Report R4, Delft Hydraulics Laboratory, Delft, The Netherlands, 14 pp.

Johnson, J.W., 1939. Discussion of 'Laboratory investigation of flume traction and transportation'. Trans. Am. Soc. Civil Eng. 104, 1247–1313.

Julien, P.Y., 1998. Erosion and Sedimentation. Cambridge University Press, New York.

Kellerhals, R., Bray, D.I., 1971. Sampling procedures for coarse fluvial sediments. J. Hydraul. Div. 97 (8), 1165–1180.

Kramer, H., 1934. Sand mixtures and sand movements in fluvial models. Proc. Am. Soc. Civil Eng. 60 (4), 443–483.

Lane, E.W., Carlson, E.J., 1953. Some factors affecting the stability of canals constructed in coarse granular materials. In: Proceedings of the 5th Congress IAHR, Delf, The Netherlands.

López, R., Justribó, C., 2010. The hydrological significance of mountains: a regional case study, the Ebro River basin, northeast Iberian Peninsula. Hydrol. Sci. J. 55 (2), 223–233.

Martin, Y., 2003. Evaluation of bed load transport formulae using field evidence from the Vedder River, British Columbia. Geomorphology 53, 75–95.

Martin, Y., Ham, D., 2005. Testing bed load transport formulae using morphologic transport estimates and field data: lower Fraser River, British Columbia. Earth Surf. Process. Land. 30, 1265–1282.

Meyer-Peter, E., Müller, R., 1948. Formulas for bed-load transport. In: Proc. 2nd Meeting of the Int. Assoc. for Hydraulic Structures Res. IAHR, Delft, The Netherlands, pp. 39–64.

Parker, G., 1990. Surface-based bedload transport relation for gravel rivers. J. Hydraul. Res. 28, 417–436.

Parker, G., Klingeman, P.C., 1982. On why gravel bed streams are paved. Water Resour. Res. 18 (5), 1409–1423.

Parker, G., Klingeman, P.C., McLean, D.G., 1982. Bedload and the size distribution of paved gravel-bed streams. J. Hydraul. Div. 108 (4), 544–571.

Recking, A., 2010. A comparison between flume and field bed load transport data and consequences for surface based bed load transport prediction. Water Resour. Res. 46, W03518. http://dx.doi.org/10.1029/2009WR008007.

Reid, I., Powell, D.M., Laronne, J.B., 1996. Prediction of bed load transport by desert flash-floods. J. Hydraul. Eng. 122 (3), 170–173.

Rice, S., Church, M., 1996. Sampling surficial fluvial gravels: the precision of size distribution percentile estimates. J. Sediment. Res. 66 (3), 654–665.

Rice, S.P., Haschenburger, J.K., 2004. A hybrid method for size characterization of coarse subsurface fluvial sediments. Earth Surf. Process. Land. 29, 373–389.

Rottner, J., 1959. A formula for bed load transportation. La Houille Blanche 3 (4), 301–307.

Shields, A., 1936. Anwendung der Aehnlichkeitsmechanik und der Turbulenzforschung auf die Geschiebebewegung, Mitteilungen der Preussischen Versuchsanstalt für Wasserbau und Schiffbau, 26, 26 pp.

Schoklitsch, A., 1950. Handbuch des wasserbaues. Springer, New York.

Shulits, S., Hill, R.D., 1968. Bed Load Formulas. Rep. No. ARSSCW-1, Agricultural Research Services, USDA, Washington.

Turowski, J.M., Badoux, A., Rickenmann, D., 2011. Start and end of bed load transport in gravel-bed streams. Geophys. Res. Lett. 38, L04401.

USACE, 1989. Sedimentation Investigations of Rivers and Reservoirs. Engineer Manual 1110-2-4000. Department of the Army, U.S. Army Corps of Engineers, Washington.

USWES, 1935. Study of River-Bed Material and Their Use with Special Reference to the Lower Mississippi River. United States Waterways Experiment Station, Vicksburg, MS, Paper 17, 161 pp.

Vericat, D., Batalla, R.J., 2005. Bed load variability under low sediment transport conditions in the lower Ebro River (NE Spain). In: Batalla, R.J., Garcia, C. (Eds.), Geomorphological Processes and Human Impacts in Rivers Basins. IAHS Publication, Wallingford, pp. 73–180.

Vericat, D., Batalla, R.J., 2006. Sediment transport in a large impounded river: the lower Ebro, NE Iberian Peninsula. Geomorphology 79, 72–92.

Vericat, D., Batalla, R.J., Garcia, C., 2006a. Breakup and reestablishment of the armor layer in a highly regulated large gravel-bed river: the lower Ebro. Geomorphology 76, 122–136.

Vericat, D., Church, M., Batalla, R.J., 2006b. Bed load bias: comparison of measurements obtained using two (76 and 152 mm) Helley–Smith samplers in a gravel-bed river. Water Resour. Res. W01402. http://dx.doi.org/10.1029/2005WR004025.

White, W.R., Milli, H., Crabbe, A.D., 1973. Sediment transport: an appraisal of available methods, Rep. 119, UK Hydraulics Research Station, Wallingford, UK.

White, W.R., Milli, H., Crabbe, A.D., 1975. Sediment transport theories: a review. Proc. Inst. Civil Eng. 59 (2), 265–292.

Wilcock, P.R., 2001. The flow, the bed, and the transport: interaction in flume and field. In: Mosley, M.P. (Ed.), Gravel-Bed Rivers V. NZHS, Wellington, NZ, pp. 183–219.

Wolman, M.G., 1954. A method of sampling coarse bed material. Am. Geophys. Union Trans. 35, 951–956.

Wong, M., Parker, G., 2006. Reanalysis and correction of bed-load relation of Meyer-Peter and Müller using their own database. J. Hydraul. Eng. 132 (11), 1159–1168.

Yang, C.T., 1973. Incipient motion and sediment transport. J. Hydraul. Div. 99 (10), 1679–1704.

Yang, C.T., 1984. Unit stream power equation for gravel. J. Hydraul. Div. 110 (12), 1783–1797.

Yang, C.T., Wan, S., 1991. Comparisons of selected bed-material load formulas. J. Hydraul. Eng. 117 (8), 973–989.